

Differentially Private Optimization on Large Model at Small Cost

Zhiqi Bu¹ Yu-Xiang Wang^{1,2} Sheng Zha¹ George Karypis¹

¹ AWS AI ² UC Santa Barbara

zhiqibu@amazon.com yuxiangw@cs.ucsb.edu
zhasheng@amazon.com gkarypis@amazon.com

Abstract

Differentially private (DP) optimization is the standard paradigm to learn large neural networks that are accurate and privacy-preserving. The computational cost for DP deep learning, however, is notoriously heavy due to the per-sample gradient clipping. Existing DP implementations are $2 - 1000\times$ more costly in time and space complexity than the standard (non-private) training. In this work, we develop a novel Book-Keeping (BK) technique that implements existing DP optimizers (thus achieving the same accuracy), with a substantial improvement on the computational cost. Specifically, BK enables DP training on large models and high dimensional data to be roughly as efficient as the standard training, whereas previous DP algorithms can be inefficient or incapable of training due to memory error. The computational advantage of BK is supported by the complexity analysis as well as extensive experiments on vision and language tasks. Our implementation achieves state-of-the-art (SOTA) accuracy with very small extra cost: on GPT2 and at the same memory cost, BK has $1.0\times$ the time complexity of the standard training ($0.75\times$ training speed in practice), and $0.6\times$ the time complexity of the most efficient DP implementation ($1.24\times$ training speed in practice). We will open-source the codebase for the BK algorithm.

1 Introduction

Deep learning with differential privacy (DP; Dwork et al. (2006)) has shown strong performance while guaranteeing rigorous protection against privacy risks, especially on large models that tend to memorize and leak the training data Carlini et al. (2021); Haim et al. (2022); Shokri et al. (2017). For example, recent advances have shed light on the success of DP GPT2 Li et al. (2021); Bu et al. (2022b); Yu et al. (2021), which achieves 64.6 BLEU score¹ at strong privacy guarantee ($\epsilon = 3$), on the text generation task using E2E restaurant review dataset. This is only marginally below the standard non-private GPT2 (BLEU score 66.8). Similarly, on computer vision tasks ($\epsilon = 2$), DP vision transformers and ResNets have obtained 97.1%/86.2% accuracy on CIFAR10/100 by Bu et al. (2022a) and over 81% accuracy on ImageNet by De et al. (2022); Mehta et al. (2022).

However, DP training of large neural networks is well-known to be computationally burdensome in comparison to the standard training, in terms of both the training time and the memory cost. For instance, training a small recurrent neural network (0.598M parameters) experiences a $1000\times$ slowdown using DP optimizers in Tensorflow-Privacy (TF-Privacy) library Bu et al. (2021), and training a small convolutional neural network (CNN, 0.605M parameters) on CIFAR10 has a $24\times$ slowdown with Tensorflow 2 and the XLA compiler Subramani et al. (2021). Even with SOTA efficient implementations, large models such as RoBERTa Liu et al. (2019), GPT2 Radford et al. (2019), ResNet He et al. (2016), VGG Simonyan & Zisserman (2014), ViT Dosovitskiy et al. (2020) and its variants, experience about $2 - 3\times$ slowdown in Pytorch Li et al. (2021);

¹BLEU (BiLingual Evaluation Understudy) is a metric (0-100) for automatically evaluating translated text. BLEU > 60 is considered as "very high quality, adequate, and fluent translations, often better than human".

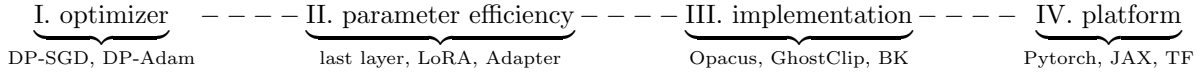
Bu et al. (2022a) and $2 - 9\times$ slowdown in JAX Kurakin et al. (2022); De et al. (2022), with possibly $4 - 20\times$ memory overhead Bu et al. (2022a); Li et al. (2021); Subramani et al. (2021) if not out of memory.

The efficiency bottleneck in DP deep learning lies in the per-sample gradient clipping, which restricts the magnitude of each per-sample gradient in the mini-batch. Applying the clipping jointly with the Gaussian noise addition, one can privately release the gradient to arbitrary optimizers like SGD and Adam, and thus guarantee the privacy of the training as described in Section 1.3:

$$\begin{aligned} \text{private gradient: } \quad \mathbf{G} &:= \sum_i \mathbf{g}_i \cdot C(\|\mathbf{g}_i\|_2) + \sigma_{\text{DP}} \cdot \mathcal{N}(0, \mathbf{I}), \\ \text{private optimizer (e.g. SGD): } \quad \mathbf{w}_{t+1} &= \mathbf{w}_t - \eta \mathbf{G}. \end{aligned} \tag{1}$$

Here \mathbf{w} is the model parameters, \mathcal{L}_i is the per-sample loss, $\mathbf{g}_i = \frac{\partial \mathcal{L}_i}{\partial \mathbf{W}}$ is the per-sample gradient, η is the learning rate, σ_{DP} is the noise magnitude that defines the privacy loss, and $C(\|\mathbf{g}_i\|)$ or simply C_i is the per-sample clipping factor, e.g. $\min\{R/\|\mathbf{g}_i\|, 1\}$ in Abadi et al. (2016), with a clipping threshold R .

At high level, previous work have tackled the efficiency bottleneck with various approaches.



One approach (part II) focuses on the parameter efficiency by partially training a neural network, in contrast to full fine-tuning all model parameters, e.g. only the last output layer Tramer & Boneh (2020), the adapter layers Houlsby et al. (2019); Mahabadi et al. (2021), or the Low-Rank Adaptation (LoRA) Hu et al. (2021); Yu et al. (2021). For example, Mehta et al. (2022) accelerate the DP training on ImageNet Deng et al. (2009) up to $30\times$ by only training the last layer of ResNet152. Noticeably, parameter efficient fine-tuning does not improve on the efficiency in terms of complexity per parameter, rather than reducing the number of parameters. Furthermore, this approach oftentimes leads to some accuracy degradation compared to DP full fine-tuning Bu et al. (2020); Mehta et al. (2022); Li et al. (2021); Yu et al. (2021).

An orthogonal approach, including this work, focuses on the computation efficiency (part III), i.e. reducing the time and space complexity through efficient implementations, without affecting the DP optimizers (part I) and thus their performance. We will elaborate on multiple methods in Section 1.2. Additionally, these methods can be compiled on different platforms (part IV) such as Tensorflow 2(XLA), JAX and Pytorch Li et al. (2021); Subramani et al. (2021); De et al. (2022); Kurakin et al. (2022), where remarkable speed difference has been observed in some cases, even with the same implementation. For example, Subramani et al. (2021) implemented DP-SGD using JAX and claimed its efficiency advantage over the same algorithm using Tensorflow or Pytorch.

1.1 Contributions

1. **[Algorithm]** We propose the book-keeping (BK) algorithm that makes existing DP optimizers fast and memory efficient, especially comparable to non-private optimizers. We demonstrate BK via the computation graph in Figure 1. The highlight is that BK *only uses one back-propagation* and *never instantiates per-sample gradients* $\{\frac{\partial \mathcal{L}_i}{\partial \mathbf{W}}\}_{i=1}^B$.
2. **[Analysis]** We analyze the complexity to show that *BK has almost the same time and space complexity as non-DP training*, especially when the feature dimension is small (see Table 5).
3. **[Extension]** We strengthen BK using a layerwise decision to mix with Opacus (see Section 3.2), which proves to be efficient when the feature dimension is large (and difficult for GhostClip). We also extend BK to the parameter efficient fine-tuning such as DP LoRA and Adapter.
4. **[Codebase]** We develop a Pytorch (Paszke et al., 2019) codebase for our BK algorithm, leveraging the auto-differentiation technique on the computation graph and a new trick in Appendix D.2.
5. **[Experiments]** We demonstrate the amazing efficiency of BK on training large models, saving the memory up to $10\times$ and boosting the speed by $30\% - 5\times$ than previous DP implementations.

Dataset	SOTA setting	Model	Time /Epoch	Relative Speed		
				over GhostClip	over Opacus	over non-DP
QQP	Li et al. (2021)	RoBERTa-large (355M)	70:04	1.36×	1.96×	0.77×
E2E	Li et al. (2021)	GPT2-large (774M)	11:20	1.24×	3.88×	0.73×
CIFAR	Bu et al. (2022a)	BEiT-large (304M)	6:35	1.33×	38.3×	0.76×

Table 1: Efficiency on tasks with SOTA DP accuracy (1 Nvidia A100 GPU; extended in Table 9).

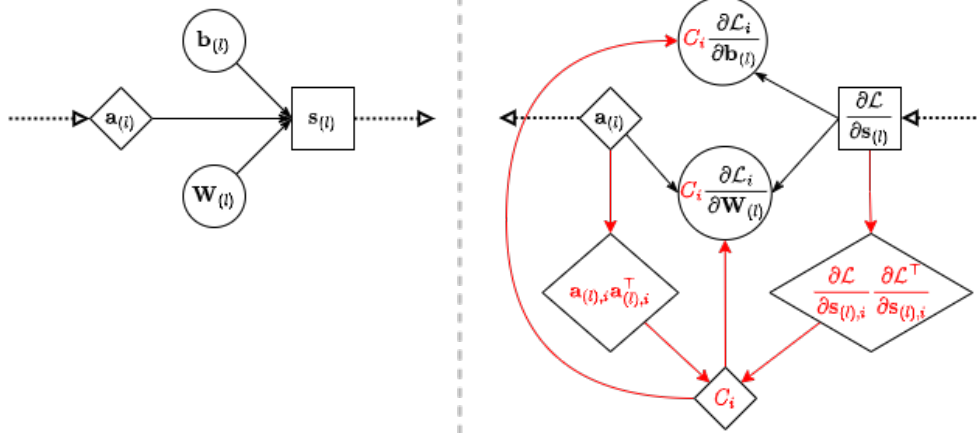


Figure 1: Forward pass and back-propagation of the l -th linear layer (standard training is in black; DP training by our book-keeping algorithm is added in red). Here $\mathbf{a}_{(l)}$ is the activation tensor, $\mathbf{s}_{(l)}$ is the layer output, $\mathbf{W}_{(l)}$, $\mathbf{b}_{(l)}$ are weight and bias, \mathcal{L}_i , \mathcal{L} are the per-sample loss and the summed loss. The dotted arrow represents the inter-layer operation such as activation, pooling, or normalization.

1.2 Related works

Previous arts have developed different implementations of the same DP optimizer in Equation (1). TF-Privacy Tensorflow back-propagates a vectorized loss $[\mathcal{L}_1, \dots, \mathcal{L}_B]$ to compute the per-sample gradients, each from one back-propagation, which is memory-efficient but slow. Opacus Yousefpour et al. (2021) and Rochette et al. (2019) accelerate the training significantly using the outer product trick in Goodfellow et al. (2014), though incurring heavy memory burden so as to store the per-sample gradients. This memory burden is partially alleviated in FastGradClip Lee & Kifer (2020) by sharing the space complexity in two rounds of back-propagation, hence almost doubling the time complexity. In ghost clipping Goodfellow (2015); Li et al. (2021); Bu et al. (2022a), the per-sample gradients can be clipped without being instantiated, thus both time and space complexity can be further improved if the feature dimension is small. We refer interested readers to Figure 3 and Appendix C for algorithmic details of these implementations.

We now compare BK to different implementations in Table 2 and Figure 2. In what follows, B is the batch size², $T_{(l)}$ is the feature dimension³, $d_{(l)}, p_{(l)}$ are the input or output dimension of a layer.

1.3 Preliminaries

We work with the (ϵ, δ) -DP by Dwork et al. (2006), which makes it difficult for any privacy attacker to distinguish or detect an arbitrary training sample, even with full access to the model (see Appendix A for details). In deep learning, DP is achieved by training on the private gradient in Equation (1) with any optimizer such as SGD, Adam, FedAvg, etc. Essentially, the private gradient is the addition of Gaussian noise to the sum of clipped per-sample gradients, which guarantees the DP protection through the privacy

²We report the physical batch size, which affects the efficiency; the accuracy is only affected by the logical batch size, which can be implemented through the gradient accumulation of physical batch size.

³For non-sequential data, $T = 1$; for texts, T is the sequence length, which is layer-independent; for images (or videos), $T_{(l)}$ is the height \times width \times time of hidden feature representation, which is layer-dependent.

	Non-DP	TF-privacy	Opacus	FastGradClip	GhostClip	BK (ours)
Instantiating per-sample grad	✗	✓	✓	✓	✗	✗
Storing every layer's grad	✗	✗	✓	✗	✗	✗
Instantiating non-DP grad	✓	✓	✓	✗	✓	✗
Number of back-propagation	1	<i>B</i>	1	<i>2</i>	<i>2</i>	1
Time Complexity of Clipping	$6BTpd$	$6BTpd$	$8BTpd$	$8BTpd$	$10BTpd + O(BT^2)$	$6BTpd + O(BT^2)$
Memory Overhead to non-DP	0	0	<i>Bpd</i>	<i>Bpd</i>	$2BT^2$	$2BT^2$
Scalable to large model	✓	✗	✗	✗	✓	✓
Scalable to high-dim input	✓	✗	✓	✓	✗	✓

Table 2: Summary of different DP implementations on a linear/convolution layer $\mathbb{R}^{B \times T_{(l)} \times d_{(l)}} \rightarrow \mathbb{R}^{B \times T_{(l)} \times p_{(l)}}$. The main bottleneck is marked in **red**.

accounting theorems Abadi et al. (2016); Mironov (2017); Dong et al. (2019); Zhu et al. (2021); Gopi et al. (2021); Koskela et al. (2020).

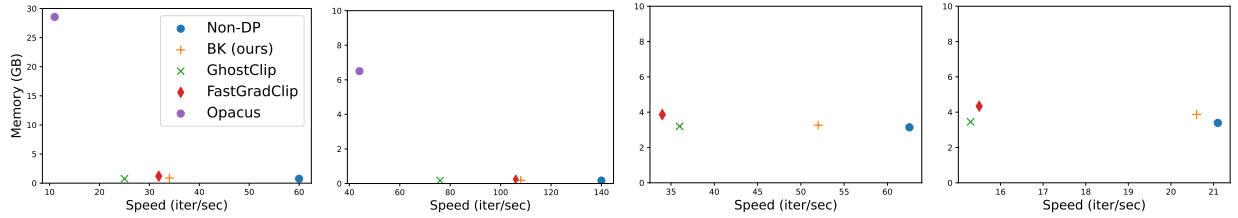


Figure 2: Speed and memory on MLP and CIFAR100 (images are flattened into vectors). Left to right: deep network (50 layers, width 1000, 50M parameters, batch size 128), shallow network (10 layers, width 1000, 10M parameters, batch size 128), and wide network (10 layers, width 5000, 250M parameters, batch size 128 or 1024; Opacus is OOM). See more ablation study in Appendix F.

2 Book-keeping: Efficient DP training in low dimension

The main computational bottleneck of DP training comes from the per-sample gradient clipping, or from the computation of per-sample gradient norms, to be exact. One widely used approach in Opacus, TF-privacy, and FastGradClip, is to instantiate the per-sample gradients and then deriving their norms. Straight-forward implementation of this approach on a mini-batch of per-sample losses requires B rounds of back-propagation (unacceptable slowdown) or $B \times$ gradient storage (unacceptable memory burden; see Opacus in Figure 2). Consequently, these implementations are not suitable for large model training. For instance, Li et al. (2021) shows that, when training GPT2-large (774M parameters), Opacus Yousefpour et al. (2021) and JAX Subramani et al. (2021) cannot fit even one single sample into a 16GB GPU.

An alternative approach, termed as the ghost clipping (GhostClip), directly computes the per-sample gradient norms without computing the gradients themselves. This is made possible, unfortunately, through two rounds of back-propagation. During the first back-propagation, one uses the regular loss $\sum_i \mathcal{L}_i$ and extracts the activation tensor and the output gradient $(\mathbf{a}, \frac{\partial \mathcal{L}}{\partial \mathbf{s}})$. One can use an algebraic trick in Equation (2) to compute the per-sample gradient norms $\{\|\frac{\partial \mathcal{L}_i}{\partial \mathbf{W}}\|_i\}$ and the clipping factors $\{C_i\}_i$ in Equation (1). During the second back-propagation, one uses the reweighted loss $\sum_i C_i \mathcal{L}_i$ whose gradient is directly the weighted gradient $\sum_i C_i \mathbf{g}_i$, which constitutes the private gradient we need. Note that this double back-propagation roughly doubles the training time (or to be more precise, $10/6 \approx 1.667 \times$ when T is small; see Table 2).

To make the DP training as efficient as the standard training, we propose the book-keeping technique (BK) that $\langle 1 \rangle$ only requires a single back-propagation, like Opacus and standard training; $\langle 2 \rangle$ does not instantiate the per-sample gradients, like GhostClip.

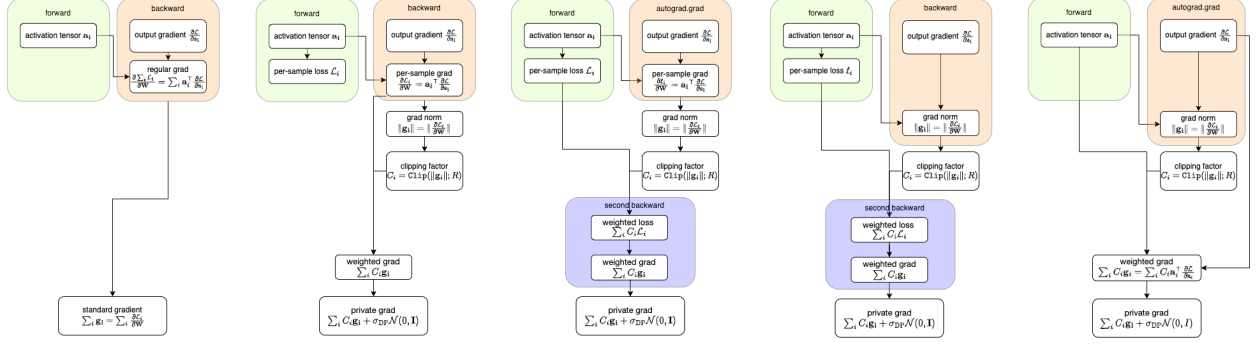


Figure 3: Standard (non-DP), Opacus, FastGradClip, GhostClip, BK implementations. Notice that BK learns to directly compute weighted gradient from Opacus, to compute the ghost norm from GhostClip, to use auto-differentiation instead of full back-propagation from FastGradClip.

2.1 Book-keeping algorithms

BK algorithms in their base forms are built on GhostClip and especially the *ghost norm* trick, so as to avoid instantiating the memory costly per-sample gradients: as can be seen in Algorithm 1 and Figure 3, $\frac{\partial \mathcal{L}_i}{\partial \mathbf{W}} = \mathbf{a}_i^\top \frac{\partial \mathcal{L}}{\partial \mathbf{s}_i}$ is not computed throughout the training. In comparison to GhostClip, our significant improvement is solely on the speed (see Table 2) through two novel tricks: the *book-keeping* and the *ghost differentiation*. The entire BK algorithm is built on the understanding of computation graph in Appendix A. Note that these tricks also offer improved efficiency for existing implementations, to be presented in Section 2.4. We now elaborate on these tricks.

$$\text{BK (base)} = \underbrace{\text{ghost norm}}_{\text{from GhostClip}} + \underbrace{\text{book-keeping}}_{\text{ours}} + \underbrace{\text{ghost differentiation}}_{\text{ours}}$$

Algorithm 1 Differentially private deep learning with BK algorithm (one iteration)

Parameters: l -th layer weights $\mathbf{W}_{(l)}$, number of layers L , noise level σ .

- 1: **for** layer $l \in 1, 2, \dots, L$ **do**
 - 2: Get activation tensor $\{\mathbf{a}_{(l),i}\}$ by Pytorch forward hook
 - 3: **for** layer $l \in L, L-1, \dots, 1$ **do**
 - 4: Get output gradient $\{\frac{\partial \mathcal{L}}{\partial \mathbf{s}_{(l),i}}\}$ by Pytorch backward hook
 - 5: Compute per-example gradient norm $\|\frac{\partial \mathcal{L}_i}{\partial \mathbf{W}_{(l)}}\|_F^2$ by ghost norm trick in Equation (2)
 - 6: Aggregate gradient norm across all layers: $\|\frac{\partial \mathcal{L}_i}{\partial \mathbf{W}}\|_F^2 = \sum_l \|\frac{\partial \mathcal{L}_i}{\partial \mathbf{W}_{(l)}}\|_F^2$
 - 7: Compute clipping factor: $C_i = C(\|\frac{\partial \mathcal{L}_i}{\partial \mathbf{W}}\|_F; R)$
 - 8: **for** layer $l \in L, L-1, \dots, 1$ **do**
 - 9: Compute sum of clipped gradients $\mathbf{G}_l = \mathbf{a}_{(l)}^\top \text{diag}(C_1, C_2, \dots) \frac{\partial \mathcal{L}}{\partial \mathbf{s}_{(l)}}$
 - 10: Delete $\{\mathbf{a}_{(l),i}\}, \{\frac{\partial \mathcal{L}}{\partial \mathbf{s}_{(l),i}}\}$
 - 11: Add Gaussian noise $\hat{\mathbf{G}} = \mathbf{G} + \sigma R \cdot \mathcal{N}(0, \mathbf{I})$
 - 12: Apply SGD/Adam/LAMB with the private gradient $\hat{\mathbf{G}}$ on \mathbf{W}
-

Ghost norm trick The ghost norm trick Goodfellow (2015) computes the gradient norm without the gradient: while the gradient is instantiated by the multiplication in Equation (2), the gradient norm can be computed without \mathbf{a}_i meeting $\frac{\partial \mathcal{L}}{\partial \mathbf{s}_i}$. This is applicable to generalized linear layers including the linear, the embedding Li et al. (2021), and the convolution layers Bu et al. (2022a). We demonstrate this trick using a simple linear layer $\mathbf{s}_i = \mathbf{a}_i \mathbf{W}$, where $\mathbf{W} \in \mathbb{R}^{d \times p}$ is the weight matrix, $\mathbf{a} \in \mathbb{R}^{B \times T \times d}$ is the mini-batch input

of this layer (a.k.a. the activation tensor) and $\mathbf{s} \in \mathbb{R}^{B \times T \times p}$ is the output. Given that the output gradient $\frac{\partial \mathcal{L}}{\partial \mathbf{s}}$ is readily available in the back-propagation, for DP and standard training, one can directly derive the per-sample gradient norm

$$\left\| \frac{\partial \mathcal{L}_i}{\partial \mathbf{W}} \right\|_{\text{Frobenius}}^2 = \text{vec} \left(\frac{\partial \mathcal{L}}{\partial \mathbf{s}_i} \frac{\partial \mathcal{L}}{\partial \mathbf{s}_i}^\top \right) \text{vec} (\mathbf{a}_i \mathbf{a}_i^\top) \text{ without computing } \frac{\partial \mathcal{L}_i}{\partial \mathbf{W}} = \mathbf{a}_i^\top \frac{\partial \mathcal{L}}{\partial \mathbf{s}_i}. \quad (2)$$

Here ‘vec’ means flattening the $T \times T$ matrix to a vector. This trick is particularly efficient when T is small, reducing the space complexity from $O(Bpd)$ to $O(BT^2)$ by Table 3.

Book-keeping trick This trick improves the time complexity by removing the second back-propagation from GhostClip. Our idea is to book-keep and re-use the output gradient $\frac{\partial \mathcal{L}}{\partial \mathbf{s}_{(l)}}$, which is deleted after the first back-propagation of GhostClip and must be re-computed during the second back-propagation. The difference between GhostClip and BK is clearly illustrated via a line-by-line comparison in Appendix C.1. In fact, denoting the total number of model parameters as $M = \sum_l p_{(l)} d_{(l)}$, our trick reduces the time complexity from $10BTM + O(BT^2)$ by GhostClip to $8BTM + O(BT^2)$ according to Table 3. In contrast to Opacus, which book-keeps the per-sample gradients $\mathbf{g}_i^{(l)}$ using $O(BM) = O(B \sum_l p_{(l)} d_{(l)})$ memory, we instead book-keep the output gradient with substantially cheaper $O(BT \sum_l p_{(l)})$ memory for small T .

Ghost differentiation trick This trick improves the time complexity on the first back-propagation in GhostClip, further reducing from $8BTM + O(BT^2)$ to $6BTM + O(BT^2)$ in Table 2. Our idea is to only compute the output gradient $\frac{\partial \mathcal{L}}{\partial \mathbf{s}_{(l)}}$ but not the parameter gradient $\frac{\partial \mathcal{L}}{\partial \mathbf{W}}$. To realize this, we break the $4BTM$ time complexity of the full back-propagation into two sub-processes, each of $2BTM$ complexity, and remove the unnecessary one. During the back-propagation of Opacus and GhostClip, `loss.backward()` calls `torch.autograd.backward` in the backend of Pytorch auto-differentiation Paszke et al. (2017), in order to compute both the output gradient $\frac{\partial \mathcal{L}}{\partial \mathbf{s}}$ and then the parameter gradient $\frac{\partial \mathcal{L}}{\partial \mathbf{W}} = \mathbf{a}^\top \frac{\partial \mathcal{L}}{\partial \mathbf{s}}$.

However, we can stop after we obtain $\frac{\partial \mathcal{L}}{\partial \mathbf{s}}$: we only need the output gradient to compute the clipped parameter gradient $\frac{\partial \sum_i C_i \mathcal{L}_i}{\partial \mathbf{W}}$ in Line 9 of Algorithm 1. Therefore, the ghost differentiation trick sets all parameters to not require gradients and applies `torch.autograd.grad` to replace `torch.autograd.backward`⁴ (see technical details in Appendix D.2, including the *origin parameter trick* that propagates on a computation graph where no parameters require gradients).

2.2 Complexity of DP implementations: a modular analysis

In this section, we analyze the complexity of DP implementations from their operation modules. We summarize the time and space complexity in Table 3 and give the derivation in Appendix B. We will refer to these modules by indices, e.g. ②a for the computation of output gradient.

Module	①Forward pass	②Back-propagation		③Ghost norm	④Per-sample grad instantiation	⑤Weighted sum of per-sample grad
		(a)output gradient	(b)parameter gradient			
Time complexity	$2BTpd$	$2BTpd$	$2BTpd$	$2BT^2(p+d)$	$2BTpd$	$2Bpd$
Space complexity	$pd + BTd$	$BT(p+d)$	pd	$2BT^2$	Bpd	0

Table 3: Time and space complexity of modules in DP training for one generalized linear layer.

⁴To get the output gradient, we call `torch.autograd.grad(loss, W)` and extract $\frac{\partial \mathcal{L}}{\partial \mathbf{s}}$ with Pytorch backward hooks. Similarly, FastGradClip Lee & Kifer (2020) directly calls `torch.autograd.grad(loss, s)` but spends additional memory to store \mathbf{s} during forward pass.

Now we are ready to decompose each implementation, following the flowcharts in Figure 3. Consequently, we can easily write down the complexity of different implementations in Table 2. Such a modular analysis displays the clear effects of the tricks in BK algorithm: the ghost norm trick removes the memory costly (4) from Opacus and FastGradClip; the book-keeping trick removes the (2b) in the second back-propagation of FastGradClip and GhostClip; the ghost differentiation trick removes the (2b) in the first back-propagation of Opacus and GhostClip.

- Standard (non-DP) = (1) + (2a) + (2b)
- Opacus = (1) + (2a) + (2b) + (4) + (5)
- FastGradClip = (1) + (2a) + (4) + (2a) + (2b)
- GhostClip = (1) + (2a) + (2b) + (3) + (2a) + (2b)
- BK (ours) = (1) + (2a) + (3) + (2b)

2.3 BK is optimally efficient in low dimension

When the feature dimension T is small, we claim that BK is almost as efficient as the standard non-private training, with a negligible $O(BT^2)$ time and memory overhead by Table 2:

Memory complexity: non-DP \approx BK \approx GhostClip $<$ FastGradClip \ll Opacus

Time complexity: non-DP \approx BK $<$ FastGradClip \approx Opacus $<$ GhostClip

Now, we discuss the cases where the data has low dimension and thus T is small. Generally speaking, the feature dimension $T_{(l)}$ depends on both the data and the model.

For non-sequential input and 1D audio data, $T = 1$. For sequential data such as texts (T being sentence length) or time series (T being time duration), $T_{(l)}$ is fixed across layers. In this case, BK is efficient on short-sequence datasets including GLUE Wang et al. (2019) (e.g. SST2/QNLI/MNLI/QQP) and natural language generation datasets (e.g. E2E/DART), since $T^2 \ll p_{(l)}d_{(l)}$. For instance, Yu et al. (2021); Li et al. (2021); Bu et al. (2022b) applied GPT2 on E2E dataset, which has a sequence length $T \approx 100$ and the number of parameters $p_{(l)}d_{(l)}$ per layer is 2 – 4M; Yu et al. (2021); Li et al. (2021) applied RoBERTa-large on GLUE datasets, which has a sequence length $T = 256$ and the number of parameters per layer is 1 – 4M. As illustrated in Figure 4 and Table 1 (extended in Table 9), BK improves the throughput of existing implementations by 25 – 388% on multiple language tasks in Li et al. (2021); Bu et al. (2022b), with minor memory overhead compared to GhostClip and non-private training.

However, on the convolution layers with image data, $T_{(l)}$ is the product of hidden feature sizes (c.f. (Bu et al., 2022a, Section 3)), thus $T_{(l)}$ depends on the original image size and network architecture. For example, larger kernel size/dilation/stride in convolution layer reduces $T_{(l)}$, while larger images have larger $T_{(l)}$ at each layer. Therefore, BK (and GhostClip) may suffer on when training ResNet on ImageNet (224×224), as we show in Figure 5 (see also (Bu et al., 2022a, Table 7)), although training the same network efficiently on CIFAR10/100 (32×32).

2.4 Applying our tricks to existing implementations

Our tricks in Section 2.1 can also improve other existing implementations, reducing the time complexity of GhostClip from $10BTpd + 2BT^2(p + d)$ to $6BTpd + 2BT^2(p + d)$, that of Opacus and FastGradClip from $8BTpd$ to $6BTpd$. We highlight that these improved implementations can be leveraged to design hybrid implementation in Section 3.2. In addition to DP full fine-tuning, we demonstrate in Appendix E.2 that BK can also be applied to the parameter efficient fine-tuning.

$$\begin{aligned}
\text{GhostClip} &= (1) + (2a) + (2b) + (3) + (2a) + (2b) \xrightarrow[\text{book-keeping}]{\text{ghost differentiation}} (1) + (2a) + (3) + (2b) \text{ (our BK)} \\
\text{Opacus} &= (1) + (2a) + (2b) + (4) + (5) \xrightarrow{\text{ghost differentiation}} (1) + (2a) + (4) + (5) \\
\text{FastGradClip} &= (1) + (2a) + (4) + (2a) + (2b) \xrightarrow{\text{book-keeping}} (1) + (2a) + (4) + (2b)
\end{aligned}$$

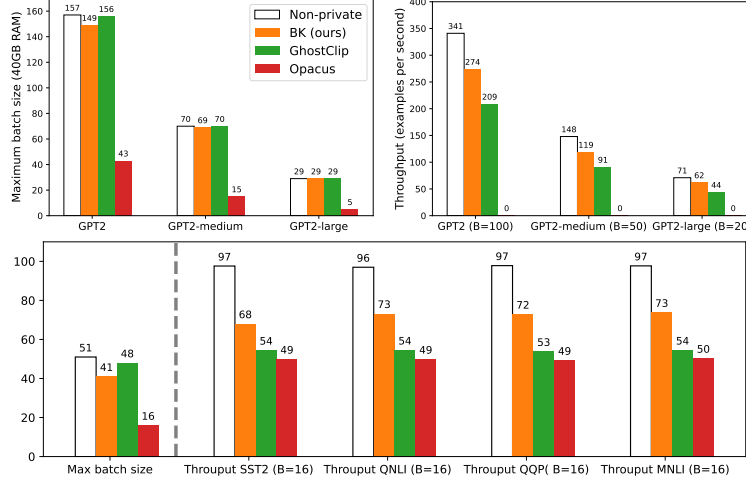


Figure 4: Memory and speed of different DP implementations. Upper: GPT2 on E2E dataset. Lower: RoBERTa-large on GLUE datasets. Note here the hybrid implementations are equivalent to the base ones, because of the short sequence length.

3 Hybrid Book-keeping: Efficient DP training in high dimension

In previous section, we have analyzed DP implementations in the small T regime, where the ghost norm-based GhostClip and BK are efficient. Nevertheless, in the large T and large model regime, none of the base implementations may be efficient (see Figure 5) and we turn to hybrid methods.

3.1 Large T necessitates non-ghost norm method

A closer look at the space complexity in Table 3 shows that, the ghost norm trick is favored over the per-sample gradient instantiation if and only if $2T_{(l)}^2 < p_{(l)}d_{(l)}$, where $p_{(l)}d_{(l)}$ is the number of parameters at one layer. When this criterion is violated for large T , GhostClip/BK can significantly under-perform Opacus/FastGradClip, as shown in Figure 5, Figure 6 and Table 10.

Similar to Section 2.3, we discuss two cases where T is large. For paragraph or document-level language tasks like WikiHop Welbl et al. (2018) and TriviaQA Joshi et al. (2017), T can range from 2000 – 20000, which makes $2T^2 = 8\text{--}800\text{M}$. For image tasks, particularly on CNN, $T_{(l)}$ varies at each layer with large values on top layers, as the features are less compressed by convolution and pooling. Taking ImageNet and the first convolution layer of VGG11 as an example (Bu et al., 2022a, Table 3), $2T_{(1)}^2 = 5 \times 10^9 \gg p_{(1)}d_{(1)} = 1.7 \times 10^3$. Consequently, ghost norm-based implementations (i.e. GhostClip and BK) costs more than 40GB memory on ResNet18, under $B = 32$, while Opacus only costs 2.5GB. This curse of dimension grows from a difficult issue on ImageNet to an impossible challenge on videos or high-resolution images, e.g. GhostClip cannot train ResNet18 with even one single CelebA-HQ image (1024×1024) using a 40GB GPU.

In short, the ghost norm trick is inefficient for large T and the per-sample gradient instantiation is inefficient for large model. Therefore, we must hybridize the base implementations.

3.2 Hybrid implementations via layerwise decision

We adopt the same layerwise decision as Bu et al. (2022a), known as the mixed ghost norm technique: we use the ghost norm trick on a layer if $2T_{(l)}^2 < p_{(l)}d_{(l)}$, and instantiate per-sample gradients otherwise. Therefore, the space complexity of computing the per-sample gradient norm reduces to $\min\{2T_{(l)}^2, p_{(l)}d_{(l)}\}$, which is significantly cheaper than either the ghost norm or the per-sample gradient instantiation in high dimension, as depicted in Table 4 and Figure 6. Consequently, over all layers, the space complexity is lower than both

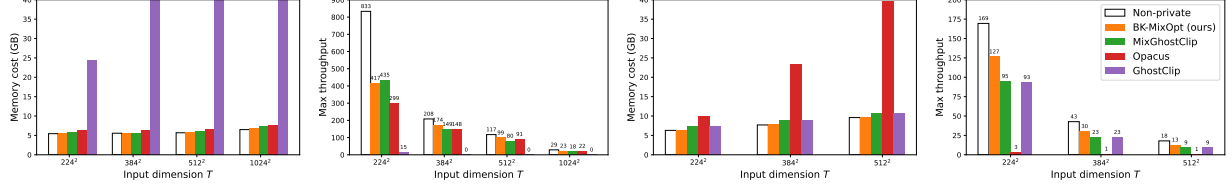


Figure 5: Memory and speed by different implementations on 50000 images. Left: VGG11 (133M;Simonyan & Zisserman (2014)), right is BEiT-large (304M;Bao et al. (2021)). Memory cost uses a physical batch size 1. Throughput uses the maximum physical batch size.

constituting methods, e.g. saving more than $10\times$ memory for the per-sample gradient clipping on ResNet18 (see more models in Table 10).

	Output size $H_{\text{out}} \times W_{\text{out}}$	Space complexity					
		18-layer		34-layer		50-layer	
		Ghost norm $2T_{(l)}^2 = 2H_{\text{out}}^2 W_{\text{out}}^2$	Per-sample grad instantiation $p_{(l)}d_{(l)} = \# \text{ params}$	Ghost norm $2T_{(l)}^2$	Per-sample grad instantiation $p_{(l)}d_{(l)}$	Ghost norm $2T_{(l)}^2$	Per-sample grad instantiation $p_{(l)}d_{(l)}$
conv1	112×112	3.1×10^8	9.4×10^3	3.1×10^8	9.4×10^3	3.1×10^8	9.4×10^3
conv2_x	56×56	$[2.0 \times 10^7] \times 4$	$[3.7 \times 10^4] \times 4$	$[2.0 \times 10^7] \times 6$	$[3.7 \times 10^4] \times 6$	$[2.0 \times 10^7] \times 9$	$[4.1 \times 10^3] \times 1$ $[3.7 \times 10^4] \times 3$ $[1.6 \times 10^4] \times 5$
conv3_x	28×28	$[1.2 \times 10^6] \times 4$	$[7.4 \times 10^4] \times 1$ $[1.5 \times 10^5] \times 3$	$[1.2 \times 10^6] \times 8$	$[7.4 \times 10^4] \times 1$ $[1.5 \times 10^5] \times 7$	$[2.0 \times 10^7] \times 1$ $[1.2 \times 10^6] \times 11$	$[3.3 \times 10^4] \times 1$ $[6.6 \times 10^4] \times 7$ $[1.5 \times 10^5] \times 4$
conv4_x	14×14	$[7.7 \times 10^4] \times 4$	$[2.9 \times 10^5] \times 1$ $[5.9 \times 10^5] \times 3$	$[7.7 \times 10^4] \times 12$	$[2.6 \times 10^5] \times 1$ $[5.9 \times 10^5] \times 11$	$[1.2 \times 10^6] \times 1$ $[7.7 \times 10^4] \times 17$	$[1.3 \times 10^5] \times 1$ $[2.6 \times 10^5] \times 11$ $[5.9 \times 10^5] \times 6$
conv5_x	7×7	$[4.8 \times 10^3] \times 4$	$[1.2 \times 10^6] \times 1$ $[2.4 \times 10^6] \times 3$	$[4.8 \times 10^3] \times 6$	$[1.2 \times 10^6] \times 1$ $[2.4 \times 10^6] \times 5$	$[4.8 \times 10^3] \times 9$	$[5.2 \times 10^5] \times 1$ $[1.0 \times 10^6] \times 5$ $[2.4 \times 10^6] \times 3$
linear	1×1	2	5.1×10^5	2	5.1×10^5	2	2.0×10^6
Total complexity		399M	11.5M	444M	21.6M	528M	22.7M
Complexity by mixed ghost norm		1.0M		2.3M		2.8M	

Table 4: Space complexity of the per-sample gradient clipping (not the entire DP algorithm) for $B = 1$ on ImageNet 224×224 . Layerwise decision of hybrid BK algorithms is highlighted in bold.

In contrast to the mixed ghost clipping (MixGhostClip) in Bu et al. (2022a), which hybridizes FastGradClip and GhostClip, we boost the efficiency by hybridizing our BK with the improved FastGradClip/Opacus in Section 2.4. We propose BK-MixOpt (and BK-MixGhostClip as an intermediate product only for comparison) and use MixGhostClip as a reference point,

- MixGhostClip = $\textcircled{1} + \textcircled{2a} + \textcircled{2b} + \min\{\textcircled{3}, \textcircled{4}\} + \textcircled{2a} + \textcircled{2b} \approx \min\{\text{GhostClip}, \text{FastGradClip}\}$,
- BK-MixGhostClip = $\textcircled{1} + \textcircled{2a} + \min\{\textcircled{3}, \textcircled{4}\} + \textcircled{2b} = \min\{\text{BK}, \text{improved FastGradClip}\}$,
- BK-MixOpt = $\textcircled{1} + \textcircled{2a} + \min\{\textcircled{3} + \textcircled{2b}, \textcircled{4} + \textcircled{5}\} = \min\{\text{BK}, \text{improved Opacus}\}$.

The hybrid BK algorithms are presented in Algorithm 5. We summarize the layerwise complexity in Table 5, from which we derive the overall complexity in Table 8 and observe that BK has almost the same complexity

as non-DP training. Note that in low dimension, the mixed ghost norm is equivalent to the ghost norm, hence MixGhostClip/BK-MixOpt is equivalent to GhostClip/BK, respectively.

Method	Type	Modification to previous variant	Time complexity	Space complexity
Non-DP			$6BTpd$	$pd + 3BTd + BTp$
Opacus	base	Instantiate per-sample gradient	$8BTpd$	$Bpd + 3BTd + BTp$
FastGradClip		Not store per-sample gradient using a second back-propagation	$8BTpd$	$Bpd + 2BTd + BTp$
GhostClip		Not instantiate per-sample gradient using ghost norm trick	$10BTpd + 2BT^2(p + d)$	$2BT^2 + 3BTd + BTp$
BK (ours)		Simplifies the two back-propagation	$6BTpd + 2BT^2(p + d)$	$2BT^2 + 3BTd + BTp$
MixGhostClip	hybrid	Mix ways to compute grad norm	$8BTpd + \langle 2BTpd, 2BT^2(p + d) \rangle$	$\min\{2BT^2, Bpd\} + 3BTd + BTp$
BK-MixGhostClip			$6BTpd + \langle 2BTpd, 2BT^2(p + d) \rangle$	$\min\{2BT^2, Bpd\} + 3BTd + BTp$
BK-MixOpt		Mix ways to compute weighted grad	$6BTpd + \langle 0, 2BT^2(p + d) \rangle$	$\min\{2BT^2, Bpd\} + 3BTd + BTp$

Table 5: Complexity of DP implementations on one layer. Here $\langle \rangle$ means between two values. The time complexity of BK-MixOpt is $6BTpd + 2BT^2(p + d) \cdot \mathbb{I}\{2T^2 < pd\}$.

3.3 Effect of model architecture & feature dimension on hybridization

We dive deeper to understand when the hybridization favors the ghost or non-ghost norm tricks.

From a model architecture viewpoint, transformers such as ViT, RoBERTa, GPT tend to prefer the ghost norm: for moderate-sequence text data and moderate-dimension image data, hybrid BK algorithms are close or equivalent to the base BK algorithm (see right-most plot in Figure 6). However, CNN prefers the per-sample gradient instantiation at top layers, and there exists a depth threshold below which the ghost norm is more efficient. Hence the hybridization is necessary to take advantages of both worlds. From the feature dimension viewpoint, larger input means this depth threshold is deeper, e.g. from the 9-th layer of ResNet18 to the 17-th layer in Figure 6, when the image size increases from 224×224 to 512×512 . We visualize this effect of feature dimension on various models in Appendix G.

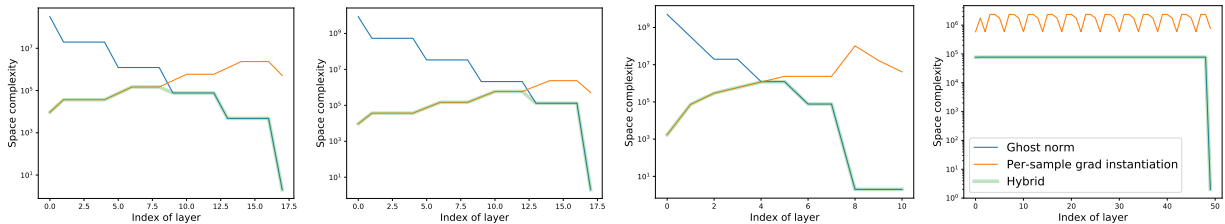


Figure 6: Layerwise space complexity of computing the per-sample gradient norm. Left to right: ResNet18 (224×224), ResNet18 (512×512), VGG11 (224×224), and ViT-base (224×224).

4 Discussion

In this work, we propose the Book-Keeping (BK) algorithms to efficiently implement DP optimizers using three tricks: ghost norm, book-keeping, and ghost differentiation. Our BK reduces the time and space complexity of DP training to the similar level of the standard training. Specially, we develop hybrid BK to overcome the computational challenge of training large models with high-dimensional data, and we extend BK to parameter efficient fine-tuning such as LoRA and Adapter.

One minor limitation of this work is that BK (and GhostClip) only applies to the weights, not the biases, of the generalized linear layers, i.e. embedding, linear, and convolution layers, though these weights constitute 99.9% of the trainable parameters (see Table 7). Implementation-wise, although BK should be

as fast as the standard training for small T , e.g. on MLP where $T = 1$, we observe some gap between the theoretical complexity and the throughput in practice. This gap is mainly due to the mechanism of Pytorch hooks which can be possibly optimized by customizing the CUDA kernel or using the symbolic programming.

References

- Martin Abadi, Andy Chu, Ian Goodfellow, H Brendan McMahan, Ilya Mironov, Kunal Talwar, and Li Zhang. Deep learning with differential privacy. In *Proceedings of the 2016 ACM SIGSAC conference on computer and communications security*, pp. 308–318, 2016.
- Hangbo Bao, Li Dong, Songhao Piao, and Furu Wei. Beit: Bert pre-training of image transformers. In *International Conference on Learning Representations*, 2021.
- Zhiqi Bu, Jinshuo Dong, Qi Long, and Weijie J Su. Deep learning with gaussian differential privacy. *Harvard data science review*, 2020(23), 2020.
- Zhiqi Bu, Sivakanth Gopi, Janardhan Kulkarni, Yin Tat Lee, Hanwen Shen, and Uthaiapon Tantipongpipat. Fast and memory efficient differentially private-sgd via jl projections. *Advances in Neural Information Processing Systems*, 34, 2021.
- Zhiqi Bu, Jialin Mao, and Shiyun Xu. Scalable and efficient training of large convolutional neural networks with differential privacy. *arXiv preprint arXiv:2205.10683*, 2022a.
- Zhiqi Bu, Yu-Xiang Wang, Sheng Zha, and George Karypis. Automatic clipping: Differentially private deep learning made easier and stronger. *arXiv preprint arXiv:2206.07136*, 2022b.
- Nicholas Carlini, Florian Tramer, Eric Wallace, Matthew Jagielski, Ariel Herbert-Voss, Katherine Lee, Adam Roberts, Tom Brown, Dawn Song, Ulfar Erlingsson, et al. Extracting training data from large language models. In *30th USENIX Security Symposium (USENIX Security 21)*, pp. 2633–2650, 2021.
- Soham De, Leonard Berrada, Jamie Hayes, Samuel L Smith, and Borja Balle. Unlocking high-accuracy differentially private image classification through scale. *arXiv preprint arXiv:2204.13650*, 2022.
- Jia Deng, Wei Dong, Richard Socher, Li-Jia Li, Kai Li, and Li Fei-Fei. Imagenet: A large-scale hierarchical image database. In *2009 IEEE conference on computer vision and pattern recognition*, pp. 248–255. Ieee, 2009.
- Jinshuo Dong, Aaron Roth, and Weijie J Su. Gaussian differential privacy. *arXiv preprint arXiv:1905.02383*, 2019.
- Alexey Dosovitskiy, Lucas Beyer, Alexander Kolesnikov, Dirk Weissenborn, Xiaohua Zhai, Thomas Unterthiner, Mostafa Dehghani, Matthias Minderer, Georg Heigold, Sylvain Gelly, et al. An image is worth 16x16 words: Transformers for image recognition at scale. In *International Conference on Learning Representations*, 2020.
- Cynthia Dwork, Frank McSherry, Kobbi Nissim, and Adam Smith. Calibrating noise to sensitivity in private data analysis. In *Theory of cryptography conference*, pp. 265–284. Springer, 2006.
- Cynthia Dwork, Aaron Roth, et al. The algorithmic foundations of differential privacy. *Found. Trends Theor. Comput. Sci.*, 9(3-4):211–407, 2014.
- Ian Goodfellow. Efficient per-example gradient computations. *arXiv preprint arXiv:1510.01799*, 2015.
- Ian J Goodfellow, Jonathon Shlens, and Christian Szegedy. Explaining and harnessing adversarial examples. *arXiv preprint arXiv:1412.6572*, 2014.
- Sivakanth Gopi, Yin Tat Lee, and Lukas Wutschitz. Numerical composition of differential privacy. *Advances in Neural Information Processing Systems*, 34, 2021.
- Niv Haim, Gal Vardi, Gilad Yehudai, Ohad Shamir, and Michal Irani. Reconstructing training data from trained neural networks. *arXiv preprint arXiv:2206.07758*, 2022.

- Kaiming He, Xiangyu Zhang, Shaoqing Ren, and Jian Sun. Deep residual learning for image recognition. In *Proceedings of the IEEE conference on computer vision and pattern recognition*, pp. 770–778, 2016.
- Neil Houlsby, Andrei Giurgiu, Stanislaw Jastrzebski, Bruna Morrone, Quentin De Laroussilhe, Andrea Gesmundo, Mona Attariyan, and Sylvain Gelly. Parameter-efficient transfer learning for nlp. In *International Conference on Machine Learning*, pp. 2790–2799. PMLR, 2019.
- Edward J Hu, Yelong Shen, Phillip Wallis, Zeyuan Allen-Zhu, Yuanzhi Li, Shean Wang, Lu Wang, and Weizhu Chen. Lora: Low-rank adaptation of large language models. *arXiv preprint arXiv:2106.09685*, 2021.
- Sergey Ioffe and Christian Szegedy. Batch normalization: Accelerating deep network training by reducing internal covariate shift. In *International conference on machine learning*, pp. 448–456. PMLR, 2015.
- Mandar Joshi, Eunsol Choi, Daniel S Weld, and Luke Zettlemoyer. Triviaqa: A large scale distantly supervised challenge dataset for reading comprehension. In *Proceedings of the 55th Annual Meeting of the Association for Computational Linguistics (Volume 1: Long Papers)*, pp. 1601–1611, 2017.
- Antti Koskela, Joonas Jälkö, and Antti Honkela. Computing tight differential privacy guarantees using fft. In *International Conference on Artificial Intelligence and Statistics*, pp. 2560–2569. PMLR, 2020.
- Alexey Kurakin, Steve Chien, Shuang Song, Roxana Geambasu, Andreas Terzis, and Abhradeep Thakurta. Toward training at imagenet scale with differential privacy. *arXiv preprint arXiv:2201.12328*, 2022.
- Jaewoo Lee and Daniel Kifer. Scaling up differentially private deep learning with fast per-example gradient clipping. *arXiv preprint arXiv:2009.03106*, 2020.
- Xuechen Li, Florian Tramer, Percy Liang, and Tatsunori Hashimoto. Large language models can be strong differentially private learners. *arXiv preprint arXiv:2110.05679*, 2021.
- Yinhan Liu, Myle Ott, Naman Goyal, Jingfei Du, Mandar Joshi, Danqi Chen, Omer Levy, Mike Lewis, Luke Zettlemoyer, and Veselin Stoyanov. Roberta: A robustly optimized bert pretraining approach. *arXiv preprint arXiv:1907.11692*, 2019.
- Rabeeh Karimi Mahabadi, James Henderson, and Sebastian Ruder. Compacter: Efficient low-rank hypercomplex adapter layers. *arXiv preprint arXiv:2106.04647*, 2021.
- Sébastien Marcel and Yann Rodriguez. Torchvision the machine-vision package of torch. In *Proceedings of the 18th ACM international conference on Multimedia*, pp. 1485–1488, 2010.
- Harsh Mehta, Abhradeep Thakurta, Alexey Kurakin, and Ashok Cutkosky. Large scale transfer learning for differentially private image classification. *arXiv preprint arXiv:2205.02973*, 2022.
- Ilya Mironov. Rényi differential privacy. In *2017 IEEE 30th computer security foundations symposium (CSF)*, pp. 263–275. IEEE, 2017.
- Adam Paszke, Sam Gross, Soumith Chintala, Gregory Chanan, Edward Yang, Zachary DeVito, Zeming Lin, Alban Desmaison, Luca Antiga, and Adam Lerer. Automatic differentiation in pytorch. 2017.
- Adam Paszke, Sam Gross, Francisco Massa, Adam Lerer, James Bradbury, Gregory Chanan, Trevor Killeen, Zeming Lin, Natalia Gimelshein, Luca Antiga, et al. Pytorch: An imperative style, high-performance deep learning library. *Advances in neural information processing systems*, 32, 2019.
- Alec Radford, Jeffrey Wu, Rewon Child, David Luan, Dario Amodei, Ilya Sutskever, et al. Language models are unsupervised multitask learners. *OpenAI blog*, 1(8):9, 2019.
- Gaspar Rochette, Andre Manoel, and Eric W Tramel. Efficient per-example gradient computations in convolutional neural networks. *arXiv preprint arXiv:1912.06015*, 2019.

- Reza Shokri, Marco Stronati, Congzheng Song, and Vitaly Shmatikov. Membership inference attacks against machine learning models. In *2017 IEEE symposium on security and privacy (SP)*, pp. 3–18. IEEE, 2017.
- Karen Simonyan and Andrew Zisserman. Very deep convolutional networks for large-scale image recognition. *arXiv preprint arXiv:1409.1556*, 2014.
- Pranav Subramani, Nicholas Vadivelu, and Gautam Kamath. Enabling fast differentially private sgd via just-in-time compilation and vectorization. *Advances in Neural Information Processing Systems*, 34, 2021.
- Tensorflow. Tensorflow/privacy: Library for training machine learning models with privacy for training data. URL <https://github.com/tensorflow/privacy>.
- Florian Tramer and Dan Boneh. Differentially private learning needs better features (or much more data). *arXiv preprint arXiv:2011.11660*, 2020.
- Alex Wang, Amanpreet Singh, Julian Michael, Felix Hill, Omer Levy, and Samuel R. Bowman. GLUE: A multi-task benchmark and analysis platform for natural language understanding. 2019. In the Proceedings of ICLR.
- Johannes Welbl, Pontus Stenetorp, and Sebastian Riedel. Constructing datasets for multi-hop reading comprehension across documents. *Transactions of the Association for Computational Linguistics*, 6:287–302, 2018.
- Ross Wightman. Pytorch image models. <https://github.com/rwightman/pytorch-image-models>, 2019.
- Thomas Wolf, Lysandre Debut, Victor Sanh, Julien Chaumond, Clement Delangue, Anthony Moi, Pierric Cistac, Tim Rault, Rémi Louf, Morgan Funtowicz, Joe Davison, Sam Shleifer, Patrick von Platen, Clara Ma, Yacine Jernite, Julien Plu, Canwen Xu, Teven Le Scao, Sylvain Gugger, Mariama Drame, Quentin Lhoest, and Alexander M. Rush. Transformers: State-of-the-art natural language processing. In *Proceedings of the 2020 Conference on Empirical Methods in Natural Language Processing: System Demonstrations*, pp. 38–45, Online, October 2020. Association for Computational Linguistics. URL <https://www.aclweb.org/anthology/2020.emnlp-demos.6>.
- Ashkan Yousefpour, Igor Shilov, Alexandre Sablayrolles, Davide Testuggine, Karthik Prasad, Mani Malek, John Nguyen, Sayan Ghosh, Akash Bharadwaj, Jessica Zhao, Graham Cormode, and Ilya Mironov. Opacus: User-friendly differential privacy library in PyTorch. *arXiv preprint arXiv:2109.12298*, 2021.
- Da Yu, Saurabh Naik, Arturs Backurs, Sivakanth Gopi, Huseyin A Inan, Gautam Kamath, Janardhan Kulkarni, Yin Tat Lee, Andre Manoel, Lukas Wutschitz, et al. Differentially private fine-tuning of language models. *arXiv preprint arXiv:2110.06500*, 2021.
- Yuqing Zhu, Jinshuo Dong, and Yu-Xiang Wang. Optimal accounting of differential privacy via characteristic function. *arXiv preprint arXiv:2106.08567*, 2021.

A Background

A.1 Differential privacy

We formally introduce the differential privacy (DP).

Definition A.1 (Dwork et al. (2006)). A randomized algorithm M is (ϵ, δ) -differentially private (DP) if for any two neighboring⁵ datasets S, S' , and for any event E ,

$$\mathbb{P}[M(S) \in E] \leq e^\epsilon \mathbb{P}[M(S') \in E] + \delta. \quad (3)$$

Clearly, stronger DP (smaller ϵ, δ) indicates the higher difficulty for privacy attackers to extract information from the training data.

DP can be achieved by adding Gaussian noise to a bounded-sensitivity function (Dwork et al., 2014, Theorem A.1). In deep learning, this function is the sum of per-sample gradients $\sum \mathbf{g}_i$ and the bounded sensitivity is R (that is guaranteed through the gradient clipping after which the per-sample gradient norm is at most R). Note that the Gaussian noise magnitude is proportional to the sensitivity: $\sigma_{\text{DP}} = \sigma R$ in Equation (1), and $\epsilon(\delta)$ only depends on σ , not on R . The derivation from (σ, T, p) in Algorithm 1 to ϵ can be done through various methods in Section 1.3.

A.2 Computation graph

We elaborate on the computation graph presented in Figure 1. For DP and the standard training, the forward pass is the same: we pass through the layers

$$\mathbf{a}_{(1)} \rightarrow \mathbf{s}_{(1)} \rightarrow \mathbf{a}_{(2)} \rightarrow \mathbf{s}_{(2)} \rightarrow \cdots \mathbf{a}_{(L)} \rightarrow \mathbf{s}_{(L)}$$

For the backward propagation, there are two sub-processes:

1. the computation of **output gradient** for all layers,

$$\frac{\partial \mathcal{L}}{\partial \mathbf{s}_{(1)}} \leftarrow \cdots \leftarrow \frac{\partial \mathcal{L}}{\partial \mathbf{s}_{(l)}} = \frac{\partial \mathcal{L}}{\partial \mathbf{s}_{(l+1)}} \mathbf{W}_{(l+1)} \circ \text{ReLU}'(\mathbf{s}_{(l)}) \leftarrow \cdots \leftarrow \frac{\partial \mathcal{L}}{\partial \mathbf{s}_{(L)}},$$

i.e. the output gradient meets with the weight \mathbf{W} ;

2. the computation of **parameter gradient** only for trainable parameters,

$$\frac{\partial \mathcal{L}}{\partial \mathbf{W}_{(l)}} = \frac{\partial \mathcal{L}}{\partial \mathbf{s}_{(l)}}^\top \frac{\partial \mathbf{s}_{(l)}}{\partial \mathbf{W}_{(l)}} = \frac{\partial \mathcal{L}}{\partial \mathbf{s}_{(l)}}^\top \mathbf{a}_{(l)},$$

i.e. the output gradient meets with the activation tensor \mathbf{a} .

Note that forward pass, output gradient, and parameter gradient have the same time complexity of $2BTM$ (B being the batch size, T being the feature dimension, e.g. the sequence length in texts, and M being the model size).

For example, GhostClip Li et al. (2021) and MixGhostClip Bu et al. (2022a), which use one forward pass and double backward propagation, have a time complexity of $10BTM + O(BT^2)$, while the standard training which uses one forward pass and a single backward propagation has a time complexity of $6BTM$.

⁵ S' is a neighbor of S if one can obtain S' by adding or removing one data point from S .

B Complexity analysis for one layer

Let us consider a layer without bias term for simplicity:

$$\mathbf{s} = \mathbf{a}\mathbf{W} \quad (4)$$

where $\mathbf{s} \in \mathbb{R}^{B \times T \times p}$ is the output or the pre-activation, $\mathbf{a} \in \mathbb{R}^{B \times T \times d}$ is the input or the post-activation of previous layer, and $\mathbf{W} \in \mathbb{R}^{d \times p}$ is the weight matrix. In a linear layer, d is the input dimension of the hidden feature, p is the output dimension of the hidden feature, and T is the sequence length (or 1 if the data are non-sequential). In a convolution layer, d is the product of the input channels and kernel sizes, p is the output channels, T is the height times width of the hidden representation.

We now break down the time and space complexities for each operation in the training. Notice that we focus on major complexities, e.g. ignoring cubic terms like BTp when higher order terms like $BTpd$ or BT^2p exist.

B.1 Forward pass

The complexity of forward pass is incurred by the standard matrix multiplication $\mathbf{s} = \mathbf{a}\mathbf{W}$. Since $\mathbf{a} \in \mathbb{R}^{B \times T \times d}$ and $\mathbf{W} \in \mathbb{R}^{d \times p}$, the time complexity is $2BTpd$ and the space complexity is $BTp + pd$.

B.2 Back-propagation: output gradient

The complexity to compute the output gradient is incurred by the chain rule: for a single sample,

$$\frac{\partial \mathcal{L}}{\partial \mathbf{s}_{(l-1),i}} = \underbrace{\frac{\partial \mathcal{L}}{\partial \mathbf{s}_{(l),i}}}_{\mathbb{R}^{T \times p}} \underbrace{\mathbf{W}_{(l)}^\top}_{\mathbb{R}^{p \times d}} \underbrace{\phi'(\mathbf{s}_{(l-1),i})}_{\mathbb{R}^{T \times d}}$$

where ϕ is the non-linear activation function. We compute the matrix multiplication $\frac{\partial \mathcal{L}}{\partial \mathbf{s}_{(l),i}} \mathbf{W}_{(l)}^\top$ first, with time complexity $2BTpd$ and space complexity $pd + BTd + BTp$. Then the elementwise product uses time complexity $2BTd$ and space complexity BTd .

B.3 Back-propagation: parameter gradient

This module could represent different operations in different DP implementations. In the first back-propagation of GhostClip and the only back-propagation of Opacus, it computes $\frac{\partial \mathcal{L}}{\partial \mathbf{W}} = \frac{\partial \sum_i \mathcal{L}_i}{\partial \mathbf{W}}$; in the second back-propagation of Ghost/FastGradClip/BK, it computes the clipped gradient $\frac{\partial \sum_i C_i \mathcal{L}_i}{\partial \mathbf{W}}$. Regardless of the cases, the operation always takes the same format as

$$\frac{\partial \mathcal{L}}{\partial \mathbf{W}} = \underbrace{\mathbf{a}}_{\mathbb{R}^{B \times T \times d}}^\top \underbrace{\frac{\partial \mathcal{L}}{\partial \mathbf{s}}}_{\mathbb{R}^{B \times T \times p}}.$$

In contrast to the per-sample gradient instantiation, this operation is a tensor multiplication instead of many matrix multiplication, and the output is a single pair of gradient $\mathbb{R}^{d \times p}$ instead of many per-sample gradients.

This tensor multiplication has time complexity $2BTpd$ and space complexity pd unless all per-sample gradients are stored.

B.4 Ghost norm

Ghost norm is the operation taking \mathbf{a}_i and $\frac{\partial \mathcal{L}}{\partial \mathbf{s}_i}$ as the input and outputs the per-sample gradient norm. According to Equation (2) and (Bu et al., 2022b, Appendix C.3), this operation computes $\mathbf{a}_i \mathbf{a}_i^\top$ and $\frac{\partial \mathcal{L}}{\partial \mathbf{s}_i} \frac{\partial \mathcal{L}}{\partial \mathbf{s}_i}^\top$, taking the time complexity $2BT^2d$ and $2BT^2p$ respectively, and the space complexity BT^2 for each variable. Hence total time complexity is $2BT^2(p + d)$ and total space complexity is $2BT^2$.

B.4.1 Per-sample gradient instantiation

Alternatively, one can instantiate the per-sample gradients and then compute their norms. This is different than the computation of parameter gradient in the back-propagation: that computation is an efficient tensor multiplication while this operation consists of B matrix multiplication.

$$\frac{\partial \mathcal{L}_i}{\partial \mathbf{W}} = \underbrace{\mathbf{a}_i}_{\mathbb{R}^{T \times d}} \underbrace{\frac{\partial \mathcal{L}}{\partial \mathbf{s}_i}}_{\mathbb{R}^{T \times p}} \text{ for } i \in [B].$$

This operation has time complexity $2BTpd$ and space complexity Bpd to store all per-sample gradients. Computing the norms is cheap enough to be neglected.

B.5 Weighted sum of per-sample gradient

This operation simply takes per-sample clipping factor $C_i \in \mathbb{R}$ and $\frac{\partial \mathcal{L}_i}{\partial \mathbf{W}} \in \mathbb{R}^{B \times d \times p}$ as the input, and outputs the clipped gradient $\mathbb{R}^{d \times p}$ as a weighted sum $\sum_i C_i \frac{\partial \mathcal{L}_i}{\partial \mathbf{W}}$. The time complexity is $2Bpd$ and the space complexity is 0 since the summation happens in place.

In contrast to double back-propagation, which indirectly derives the clipped gradient by differentiating the reweighted loss $\sum_i C_i \mathcal{L}_i$ at a cost of $O(BTpd)$, this operation directly computes the clipped gradient under almost no time complexity. Noticeably, this is only possible if per-sample gradients are readily instantiated and stored.

C Line-by-line comparison between different implementations

C.1 BK v.s. GhostClip

Algorithm 2 DP optimizer with BK or GhostClip

Parameters: l -th layer weights $\mathbf{W}_{(l)}$, number of layers L , noise level σ .

- 1: *# forward pass*
 - 2: **for** layer $l \in 1, 2, \dots, L$ **do**
 - 3: Get $\{\mathbf{a}_{(l),i}\}$
 - 4: *# backward propagation with loss $\mathcal{L} = \sum_i \mathcal{L}_i$*
 - 5: **for** layer $l \in L, L-1, \dots, 1$ **do**
 - 6: Get output gradient $\{\frac{\partial \mathcal{L}}{\partial \mathbf{s}_{(l),i}}\}$
 - 7: Compute per-sample gradient norm: $\|\frac{\partial \mathcal{L}_i}{\partial \mathbf{W}_{(l)}}\|_F^2 = \text{vec}(\frac{\partial \mathcal{L}}{\partial \mathbf{s}_{(l),i}}^\top \frac{\partial \mathcal{L}}{\partial \mathbf{s}_{(l),i}}) \cdot \text{vec}(\mathbf{a}_{(l),i}^\top \mathbf{a}_{(l),i})$
 - 8: Compute non-private gradient: $\frac{\partial \mathcal{L}}{\partial \mathbf{W}_{(l)}} = \mathbf{a}_{(l)}^\top \frac{\partial \mathcal{L}}{\partial \mathbf{s}_{(l)}}$
 - 9: Aggregate gradient norm across all layers: $\|\frac{\partial \mathcal{L}_i}{\partial \mathbf{W}}\|_F^2 = \sum_l \|\frac{\partial \mathcal{L}_i}{\partial \mathbf{W}_{(l)}}\|_F^2$
 - 10: Compute clipping factor: $C_i = C(\|\frac{\partial \mathcal{L}_i}{\partial \mathbf{W}}\|_F; R)$
 - 11: **for** layer $l \in L, L-1, \dots, 1$ **do**
 - 12: Compute sum of clipped gradients $\mathbf{G}_l = \mathbf{a}_{(l)}^\top \text{diag}(\mathbf{C}) \frac{\partial \mathcal{L}}{\partial \mathbf{s}_{(l)}}$
 - 13: *# 2nd backward propagation with loss $\mathcal{L} = \sum_i C_i \mathcal{L}_i$*
 - 14: Get output gradient $\{\frac{\partial \sum C_i \mathcal{L}_i}{\partial \mathbf{s}_{(l),i}}\}$
 - 15: Compute sum of clipped gradients $\mathbf{G}_l = \mathbf{a}_{(l)}^\top \frac{\partial \sum C_i \mathcal{L}_i}{\partial \mathbf{s}_{(l)}}$
 - 16: Delete $\{\mathbf{a}_{(l),i}\}, \{\frac{\partial \mathcal{L}}{\partial \mathbf{s}_{(l),i}}\}, \{\frac{\partial \sum C_i \mathcal{L}_i}{\partial \mathbf{s}_{(l),i}}\}$
 - 17: Add Gaussian noise $\hat{\mathbf{G}} = \mathbf{G} + \sigma R \cdot \mathcal{N}(0, \mathbf{I})$
 - 18: Apply SGD/Adam/LAMB with the private gradient $\hat{\mathbf{G}}$ on \mathbf{W}
-

C.2 BK v.s. Opacus

Algorithm 3 DP optimizer with BK or Opacus

Parameters: l -th layer's weights $\mathbf{W}_{(l),t}$, number of layers L , noise scale σ .

- 1: **for** layer $l \in 1, 2, \dots, L$ **do**
 - 2: Get $\{\mathbf{a}_{(l),i}\}$
 - 3: **for** layer $l \in L, L-1, \dots, 1$ **do**
 - 4: Get output gradient $\{\frac{\partial \mathcal{L}}{\partial \mathbf{s}_{(l),i}}\}$
 - 5: Compute per-sample gradient norm: $\|\frac{\partial \mathcal{L}_i}{\partial \mathbf{W}_{(l)}}\|_F^2 = \text{vec}(\frac{\partial \mathcal{L}}{\partial \mathbf{s}_{(l),i}}^\top \frac{\partial \mathcal{L}}{\partial \mathbf{s}_{(l),i}}) \cdot \text{vec}(\mathbf{a}_{(l),i}^\top \mathbf{a}_{(l),i})$
 - 6: Compute non-private gradient: $\frac{\partial \mathcal{L}}{\partial \mathbf{W}_{(l)}} = \mathbf{a}_{(l)}^\top \frac{\partial \mathcal{L}}{\partial \mathbf{s}_{(l)}}$
 - 7: Compute per-sample gradients: $\frac{\partial \mathcal{L}_i}{\partial \mathbf{W}_{(l)}} = \mathbf{a}_{(l),i}^\top \frac{\partial \mathcal{L}}{\partial \mathbf{s}_{(l),i}}$ and gradient norms $\|\frac{\partial \mathcal{L}_i}{\partial \mathbf{W}_{(l)}}\|_F^2$
 - 8: Delete $\{\mathbf{a}_{(l),i}\}, \{\frac{\partial \mathcal{L}}{\partial \mathbf{s}_{(l),i}}\}$
 - 9: Aggregate gradient norm across all layers: $\|\frac{\partial \mathcal{L}_i}{\partial \mathbf{W}}\|_F^2 = \sum_l \|\frac{\partial \mathcal{L}_i}{\partial \mathbf{W}_{(l)}}\|_F^2$
 - 10: Compute clipping factor: $C_i = C(\|\frac{\partial \mathcal{L}_i}{\partial \mathbf{W}}\|_F; R)$
 - 11: **for** layer $l \in L, L-1, \dots, 1$ **do**
 - 12: Compute sum of clipped gradients $\mathbf{G}_l = \mathbf{a}_{(l)}^\top \text{diag}(\mathbf{C}) \frac{\partial \mathcal{L}}{\partial \mathbf{s}_{(l)}}$
 - 13: Compute sum of clipped gradients $\mathbf{G}_l = \sum C_i \frac{\partial \mathcal{L}_i}{\partial \mathbf{W}_{(l)}}$
 - 14: Delete $\{\mathbf{a}_{(l),i}\}, \{\frac{\partial \mathcal{L}}{\partial \mathbf{s}_{(l),i}}\}, \{\frac{\partial \mathcal{L}}{\partial \mathbf{W}_{(l)}}\}$
 - 15: Add Gaussian noise $\hat{\mathbf{G}} = \mathbf{G} + \sigma R \cdot \mathcal{N}(0, \mathbf{I})$
 - 16: Apply SGD/Adam/LAMB with the private gradient $\hat{\mathbf{G}}$ on \mathbf{W}
-

C.3 BK v.s. standard (non-DP)

Algorithm 4 DP optimizer with BK or Standard optimizer

Parameters: l -th layer's weights $\mathbf{W}_{(l),t}$, number of layers L , noise scale σ .

- 1: **for** layer $l \in 1, 2, \dots, L$ **do**
 - 2: Get $\{\mathbf{a}_{(l),i}\}$
 - 3: **for** layer $l \in L, L-1, \dots, 1$ **do**
 - 4: Get output gradient $\{\frac{\partial \mathcal{L}}{\partial \mathbf{s}_{(l),i}}\}$
 - 5: Compute per-sample gradient norm: $\|\frac{\partial \mathcal{L}_i}{\partial \mathbf{W}_{(l)}}\|_F^2 = \text{vec}(\frac{\partial \mathcal{L}}{\partial \mathbf{s}_{(l),i}}^\top \frac{\partial \mathcal{L}}{\partial \mathbf{s}_{(l),i}}) \cdot \text{vec}(\mathbf{a}_{(l),i}^\top \mathbf{a}_{(l),i})$
 - 6: Compute non-private gradient: $\frac{\partial \mathcal{L}}{\partial \mathbf{W}_{(l)}} = \mathbf{a}_{(l)}^\top \frac{\partial \mathcal{L}}{\partial \mathbf{s}_{(l)}}$
 - 7: Delete $\{\mathbf{a}_{(l),i}\}, \{\frac{\partial \mathcal{L}}{\partial \mathbf{s}_{(l),i}}\}$
 - 8: Aggregate gradient norm across all layers: $\|\frac{\partial \mathcal{L}_i}{\partial \mathbf{W}}\|_F^2 = \sum_l \|\frac{\partial \mathcal{L}_i}{\partial \mathbf{W}_{(l)}}\|_F^2$
 - 9: Compute clipping factor: $C_i = C(\|\frac{\partial \mathcal{L}_i}{\partial \mathbf{W}}\|_F; R)$
 - 10: **for** layer $l \in L, L-1, \dots, 1$ **do**
 - 11: Compute sum of clipped gradients $\mathbf{G}_l = \mathbf{a}_{(l)}^\top \text{diag}(\mathbf{C}) \frac{\partial \mathcal{L}}{\partial \mathbf{s}_{(l)}}$
 - 12: Delete $\{\mathbf{a}_{(l),i}\}, \{\frac{\partial \mathcal{L}}{\partial \mathbf{s}_{(l),i}}\}$
 - 13: Add Gaussian noise $\hat{\mathbf{G}} = \mathbf{G} + \sigma R \cdot \mathcal{N}(0, \mathbf{I})$
 - 14: Apply SGD/Adam/LAMB with $\hat{\mathbf{G}}$ or \mathbf{G} on \mathbf{W}
-

C.4 BK (base) v.s. hybrid BK

Algorithm 5 DP optimizer with BK, BK- **MixGhostClip** or BK- **MixOpt**

Parameters: l -th layer’s weights $\mathbf{W}_{(l)}$, number of layers L , noise scale σ .

```

1: # forward pass
2: for layer  $l \in 1, 2, \dots, L$  do
3:   Get  $\{\mathbf{a}_{(l),i}\}$ 
4: # backward propagation with loss  $\mathcal{L} = \sum_i \mathcal{L}_i$ 
5: for layer  $l \in L, L-1, \dots, 1$  do
6:   Get output gradient  $\{\frac{\partial \mathcal{L}}{\partial \mathbf{s}_{(l),i}}\}$ 
7:   if (MixGhostClip or MixOpt) and  $2T_{(l)}^2 > p_{(l)}d_{(l)}$  then
8:     Compute per-sample gradients:  $\frac{\partial \mathcal{L}_i}{\partial \mathbf{W}_{(l)}} = \mathbf{a}_{(l),i}^\top \frac{\partial \mathcal{L}}{\partial \mathbf{s}_{(l),i}}$  and gradient norms  $\|\frac{\partial \mathcal{L}_i}{\partial \mathbf{W}_{(l)}}\|_F^2$ 
9:   else
10:    Compute per-sample gradient norm:  $\|\frac{\partial \mathcal{L}_i}{\partial \mathbf{W}_{(l)}}\|_F^2 = \text{vec}(\frac{\partial \mathcal{L}}{\partial \mathbf{s}_{(l),i}}^\top \frac{\partial \mathcal{L}}{\partial \mathbf{s}_{(l),i}}) \cdot \text{vec}(\mathbf{a}_{(l),i}^\top \mathbf{a}_{(l),i})$ 
11:  Aggregate gradient norm across all layers:  $\|\frac{\partial \mathcal{L}_i}{\partial \mathbf{W}}\|_F^2 = \sum_l \|\frac{\partial \mathcal{L}_i}{\partial \mathbf{W}_{(l)}}\|_F^2$ 
12:  Compute clipping factor:  $C_i = C(\|\frac{\partial \mathcal{L}_i}{\partial \mathbf{W}}\|_F; R)$ 
13:  for layer  $l \in L, L-1, \dots, 1$  do
14:    if MixOpt and  $2T_{(l)}^2 > p_{(l)}d_{(l)}$  then
15:      Compute weighted gradients  $\mathbf{G}_l = \sum C_i \frac{\partial \mathcal{L}_i}{\partial \mathbf{W}_{(l)}}$ 
16:    else
17:      Compute sum of clipped gradients  $\mathbf{G}_l = \mathbf{a}_{(l)}^\top \text{diag}(\mathbf{C}) \frac{\partial \mathcal{L}}{\partial \mathbf{s}_{(l)}}$ 
18:    Delete  $\{\mathbf{a}_{(l),i}\}, \{\frac{\partial \mathcal{L}}{\partial \mathbf{s}_{(l),i}}\}, \{\frac{\partial \mathcal{L}_i}{\partial \mathbf{W}_{(l)}}\}$ 
19:  Add Gaussian noise  $\hat{\mathbf{G}} = \mathbf{G} + \sigma R \cdot \mathcal{N}(0, \mathbf{I})$ 
20:  Apply SGD/Adam/LAMB with the private gradient  $\hat{\mathbf{G}}$  on  $\mathbf{W}$ 

```

D Codebase README

Here we describe some designs in our codebase for BK algorithms.

D.1 Supported layers

- Linear: Ghost norm or per-sample gradient instantiation
- Embedding: Ghost norm
- Conv1d&Conv2d: Ghost or per-sample gradient instantiation
- GroupNorm&LayerNorm: per-sample gradient instantiation

D.2 Instruction of implementation

In this section, we will discuss the specific designs and tricks for our book-keeping technique. We illustrate through Pytorch automatic differentiation package, known as `torch.autograd` or simply `autograd`⁶. It has two high-level operators, `autograd.backward` (which is the major component of the commonly used `loss.backward()`) and `autograd.grad`. We denote the model parameters as `param`.

⁶See <https://pytorch.org/docs/stable/autograd.html> for an official introduction.

On all trainable layers, i.e. layers with at least one trainable parameter such that `param.requires_grad=True`, the operator `autograd.backward` does three things, 1. compute the output gradient $\frac{\partial \mathcal{L}}{\partial \mathbf{s}}$ for this layer; 2. compute the parameter gradient $\frac{\partial \mathcal{L}}{\partial \mathbf{W}}$ or $\frac{\partial \mathcal{L}}{\partial \mathbf{b}}$; 3. store the parameter gradient to `param.grad` attribute.

In contrast, `autograd.grad` returns but does not store the parameter gradient in step 3, thus saving some memory cost. However, `autograd.grad` still computes the parameter gradient in step 2 (or (2b)) unnecessarily.

Therefore the key idea is to only compute the output gradient without computing the parameter gradient. This goal can be achieved by

1. registering the Pytorch backward hooks, which have free access to the output gradient $\frac{\partial \mathcal{L}}{\partial \mathbf{s}}$, to store this output gradient for (2a) (Line 9 of Algorithm 1);
2. setting all parameters to not require gradients, through `requires_grad=False`.

D.3 Work-around: origin parameters

Unfortunately, the back-propagation will not be executed if all parameters are set to not require gradients, since the computation graph needs to be created at least on some trainable parameters. Therefore, while the above methodology is certainly implementable through mild modification on the low level (like CUDA kernel), we provide a lightweight work-around in Pytorch.

To make sure that the back-propagation indeed propagates through all trainable parameters, we set `param.requires_grad=True` on and only on the ancestor parameter nodes of all output nodes, termed as the **origin parameters**. Specifically, we define the origin parameters as the *subset of parameter nodes, whose descendant nodes cover all the output nodes*. This is visualized in Figure 7 for a 3-layer MLP, using the same symbols as Figure 1.

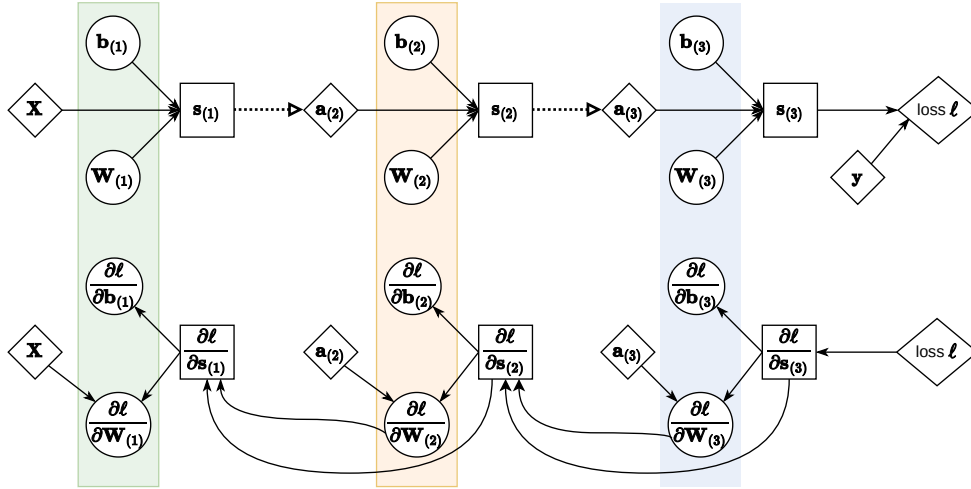


Figure 7: Forward pass (upper panel) and back-propagation (lower panel) of a 3-layer MLP.

Here, $\mathbf{s}_{(i)}$ are the output nodes (in squares) from the trainable layers. The ancestor parameter nodes (in circles) of $\mathbf{s}_{(3)}$ are $\{\mathbf{b}_{(3)}, \mathbf{b}_{(2)}, \mathbf{b}_{(1)}, \mathbf{W}_{(3)}, \mathbf{W}_{(2)}, \mathbf{W}_{(1)}\}$, those of $\mathbf{s}_{(2)}$ are $\{\mathbf{b}_{(2)}, \mathbf{b}_{(1)}, \mathbf{W}_{(2)}, \mathbf{W}_{(1)}\}$, and those of $\mathbf{s}_{(1)}$ are $\{\mathbf{b}_{(1)}, \mathbf{W}_{(1)}\}$. Therefore, subsets including but not limited to $\{\mathbf{b}_{(3)}, \mathbf{b}_{(2)}, \mathbf{b}_{(1)}, \mathbf{W}_{(3)}, \mathbf{W}_{(2)}, \mathbf{W}_{(1)}\}$, $\{\mathbf{b}_{(1)}, \mathbf{W}_{(1)}\}$, and $\{\mathbf{b}_{(1)}\}$ are qualified as the origin parameters, since their descendants cover all output nodes. In fact, the smallest subsets are $\{\mathbf{b}_{(1)}\}$ or $\{\mathbf{W}_{(1)}\}$, and either can serve as the optimal origin parameters.

Remark D.1. The origin parameters are usually within the embedding layer in language models and transformers, or within the first convolution layer in vision models. Since the origin parameters only constitute

a small fraction of all trainable parameters (fewer than the parameters in the first layer) in deep neural networks (with hundreds of layers), the computational overhead wasted on the regular gradient of origin parameters is negligible.

Remark D.2. Since we will waste the computation of regular gradient $\frac{\partial \mathcal{L}}{\partial \text{origin_parameters}}$, it is preferred to use the bias over the weight for minimum waste whenever possible. We note that sometimes the first layer contains no bias term. For example, the embedding layer by `torch.nn.Embedding` has no bias by design, and so do all convolution layers in ResNets from torchvision Marcel & Rodriguez (2010), with reasons discussed at (Ioffe & Szegedy, 2015, Section 3.2), which generalizes to all batch-normalized CNN if the normalization is applied before the activation function.

In summary, we use `torch.autograd.grad(loss, origin_parameters)` to drive the back-propagation without computing the regular parameter gradient $\frac{\partial \sum_i \mathcal{L}_i}{\partial \mathbf{W}}$ (by setting `param.requires_grad=False`), and use Pytorch backward hooks to access and store the output gradient $\frac{\partial \mathcal{L}}{\partial \mathbf{s}}$.

	non-DP training		DP training (Book-Keeping)		
	trainable param	non-trainable param	trainable param (origin param)	trainable param (not origin param)	non-trainable param
register hook	✗	✗	✓	✓	✗
<code>param.requires_grad</code>	✓	✗	✓	✗	✗

Table 6: Origin parameter trick and implementation details.

D.4 How to use BK codebase

With a few lines of code, it is easy to use our BK codebase to change the standard training to the DP training. Note that we do not call `loss.backward()` as the back-propagation is implicitly called inside the `optimizer.step(loss=loss)`.

```
from BK import PrivacyEngine
from transformers import AutoModel
import torch.nn.functional as F

model = AutoModel.from_pretrained('roberta-base')

optimizer = torch.optim.Adam(params=model.parameters())
privacy_engine = PrivacyEngine(
    model, batch_size=256, sample_size=50000, max_grad_norm=0.1,
    epochs=3, target_epsilon=3, MixGhostClip=True, MixOpt=True)
privacy_engine.attach(optimizer)

# Same training procedure, e.g. data loading, forward pass, logits...
loss = F.cross_entropy(logits, labels)
optimizer.step(loss=loss)
```

Notice that if `MixGhostClip==False` and `MixOpt==False`, then BK (base) is implemented; if `MixGhostClip==True` and `MixOpt==False`, then BK-MixGhostClip is implemented; if `MixOpt==True`, then BK-MixOpt is implemented.

We also allows the gradient accumulation through `optimizer.virtual_step(loss=loss)`, similar to Opacus v0.15.0.

E Applicability of BK algorithm

E.1 Applying BK to full fine-tuning

We experiment with numerous vision and language models to show the strong applicability of BK. Notice that the ghost norm trick only applies on weight parameters and in the generalized linear layers, i.e. embedding/convolutional/linear. The vision models are imported from Pytorch Image Models library Wightman (2019) and the language models are imported from Hugging Face Transformers library Wolf et al. (2020)⁷.

E.2 Applying BK to parameter efficient fine-tuning

We demonstrate that BK (base and hybrid) can be applied to DP LoRA and DP Adapter, where the rank r is usually 16-1024. For the ease of presentation, we describe the BK base, similarly to Algorithm 1.

Adapter An adapter module is injected after a linear layer:

$$A(x) = \tau(xD)U + x$$

where $x \in \mathbb{R}^{B \times T \times p}$, $D \in \mathbb{R}^{p \times r}$, $U \in \mathbb{R}^{r \times p}$. We decompose the module A into two sub-modules:

- $x \rightarrow xD := u$, activation x , output grad $\frac{\partial \mathcal{L}}{\partial u}$
- $\tau(u) \rightarrow \tau U := v$, activation $\tau(xD)$, output grad $\frac{\partial \mathcal{L}}{\partial v}$

Hence BK can be implemented as follows.

1. Get activation tensors x and $\tau(xD)$ by Pytorch forward hook
2. Get output gradients $\{\frac{\partial \mathcal{L}}{\partial xD}\}$ and $\{\frac{\partial \mathcal{L}}{\partial \tau U}\}$ by Pytorch backward hook
3. Compute per-example gradient norm $\|\frac{\partial \mathcal{L}_i}{\partial D}\|_F^2$ and $\|\frac{\partial \mathcal{L}_i}{\partial U}\|_F^2$ by ghost norm trick
4. Aggregate gradient norm across all layers: $\|\frac{\partial \mathcal{L}_i}{\partial D}\|_F^2 + \|\frac{\partial \mathcal{L}_i}{\partial U}\|_F^2$
5. Compute clipping factor C_i
6. Compute sum of clipped gradients $\mathbf{G}_D = x^\top \text{diag}(C_1, C_2, \dots) \frac{\partial \mathcal{L}}{\partial xD}$ and $\mathbf{G}_U = \tau^\top \text{diag}(C_1, C_2, \dots) \frac{\partial \mathcal{L}}{\partial \tau U}$
7. Add Gaussian noise $\hat{\mathbf{G}}_D = \mathbf{G}_D + \sigma R \cdot \mathcal{N}(0, \mathbf{I})$ and $\hat{\mathbf{G}}_U = \mathbf{G}_U + \sigma R \cdot \mathcal{N}(0, \mathbf{I})$
8. Apply SGD/Adam/LAMB with the private gradient $\hat{\mathbf{G}}_D$ on D and $\hat{\mathbf{G}}_U$ on U

Existing implementation of DP Adapter⁸ uses the per-sample gradient instantiation as in Opacus. It is not hard to see that the layerwise space overhead (in addition to forward pass and output gradient) is $2Bpr$ and the time overhead is $4BTpr$ (c.f. Table 3 (4)). With the BK implementation, the space overhead is $4BT^2$ and the time overhead is $4BT^2(p+r)$ (c.f. Table 3 (3)).

⁷In Transformers library, layers with class name ‘Conv1D’ is actually a linear layer, different from 1D convolution `torch.nn.Conv1d`.

⁸https://github.com/huseyinatahaninan/Differentially-Private-Fine-tuning-of-Language-Models/tree/main/Language-Understanding-RoBERTa/bert_adapter

LoRA LoRA modifies

$$A(x) = x(W + LR) = xW + xLR$$

where $x \in \mathbb{R}^{B \times T \times d}$, $W \in \mathbb{R}^{d \times p}$, $L \in \mathbb{R}^{d \times r}$, $R \in \mathbb{R}^{r \times p}$. We decompose the module A into two sub-modules:

- $x \rightarrow xL := u$, activation x , output grad $\frac{\partial \mathcal{L}}{\partial u}$
- $u \rightarrow uR := v$, activation xL , output grad $\frac{\partial \mathcal{L}}{\partial v}$

Hence BK can be implemented on each sub-module, similar to the DP Adapter.

Existing implementation of DP LoRA⁹ uses the per-sample gradient instantiation as in Opacus. It is not hard to see that the layerwise space overhead (in addition to forward pass and output gradient) is $Br(p + d)$ and the time overhead is $2BT r(p + d)$ (c.f. Table 3 (4)). With the BK implementation, the space overhead is $4BT^2$ and the time overhead is $2BT^2(p + d + 2r)$ (c.f. Table 3 (3)).

⁹https://github.com/huseyinatahaninan/Differentially-Private-Fine-tuning-of-Language-Models/tree/main/Language-Understanding-RoBERTa/bert_lora

Model	# param in generalized linear layers		# param in other layers weight+bias	% applicable to BK
	weight	bias		
ResNet18	11.7M	1000	9600	99.9%
ResNet34	21.8M	1000	17024	99.9%
ResNet50	25.5M	1000	53120	99.8%
ResNet101	44.4M	1000	105344	99.8%
ResNet152	60.2M	1000	151424	99.7%
DenseNet121	7.9M	1000	83648	98.9%
DenseNet161	28.5M	1000	219936	99.2%
DenseNet201	19.8M	1000	229056	98.9%
Wide ResNet50	68.8M	1000	68224	99.9%
Wide ResNet101	126.7M	1000	137856	99.9%
vit_tiny_patch16_224	5.6M	21928	9600	99.4%
vit_small_patch16_224	21.9M	42856	19200	99.7%
vit_base_patch16_224	86.3M	84712	38400	99.9%
vit_large_patch16_224	303.8M	223208	100352	99.9%
crossvit_tiny_240	6.9M	30800	16128	99.3%
crossvit_small_240	26.6M	59600	32256	99.7%
crossvit_base_240	104.5M	117200	64512	99.8%
convnext_small	50.1M	83656	30144	99.8%
convnext_base	88.4M	111208	40192	99.8%
convnext_large	197.5M	166312	60288	99.9%
deit_tiny_patch16_224	5.6M	21928	9600	99.4%
deit_small_patch16_224	21.9M	42856	19200	99.7%
deit_base_patch16_224	86.3M	84712	38400	99.9%
beit_base_patch16_224	86.3M	57064	38400	99.9%
beit_large_patch16_224	303.8M	149480	100352	99.9%
roberta-base	124.5M	83712	38400	99.9%
roberta-large	355.0M	222208	100352	99.9%
distilroberta-base	82.1M	42240	19968	99.9%
bert-base-uncased	109.4M	83712	38400	99.9%
bert-large-uncased	334.8M	222208	100352	99.9%
bert-base-cased	108.2M	83712	38400	99.9%
bert-large-cased	333.3M	222208	100352	99.9%
longformer-base-4096	148.5M	111360	38400	99.9%
longformer-large-4096	434.2M	295936	100352	99.9%
t5-small	60.5M	0	16384	99.9%
t5-base	222.9M	0	47616	99.98%
t5-large	737.5M	0	124928	99.98%
long-t5-local-base	222.9M	0	47616	99.98%
long-t5-local-large	750.1M	0	124928	99.98%
long-t5-tglobal-base	222.9M	0	56832	99.97%
long-t5-tglobal-large	750.1M	0	149504	99.98%
gpt2	124.3M	82944	38400	99.9%
gpt2-medium	354.5M	221184	100352	99.9%
gpt2-large	773.4M	414720	186880	99.9%

Table 7: Models and the percentage of trainable parameters in generalized linear layers.

F Additional plots and tables

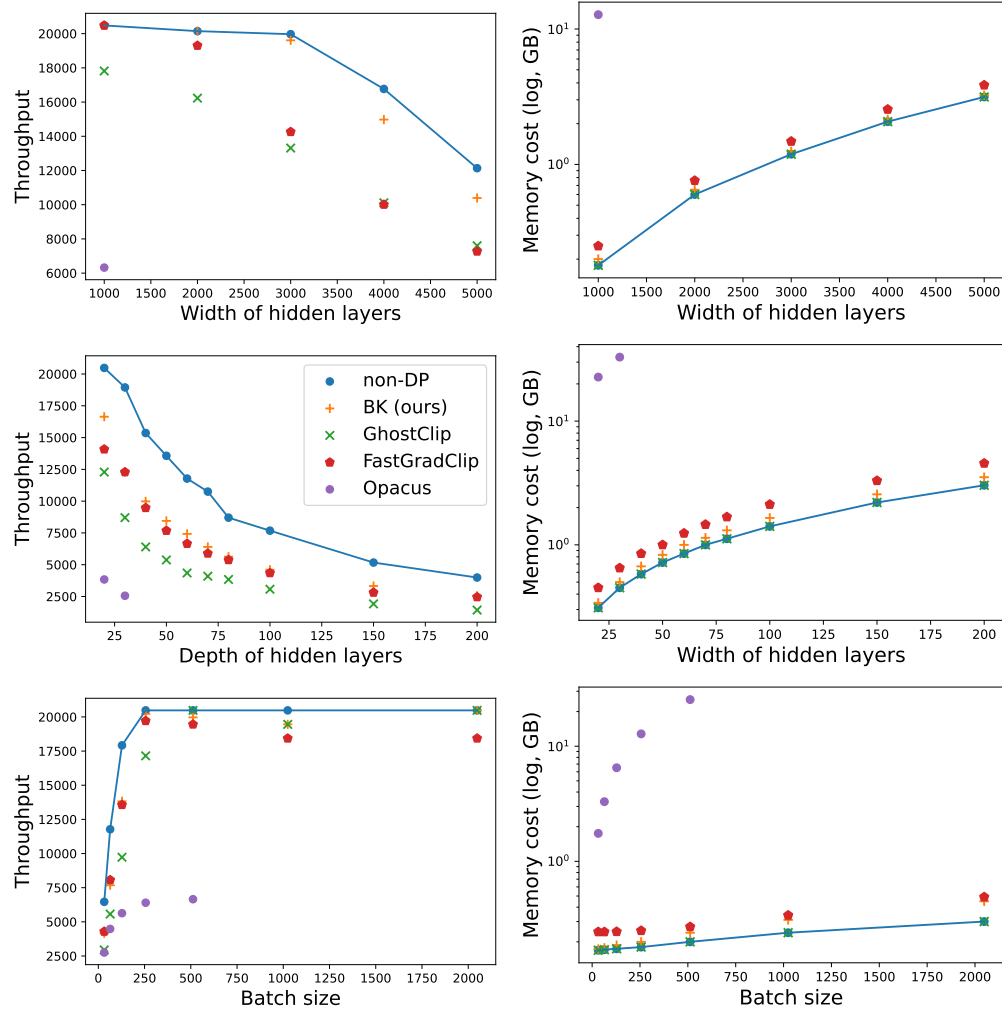


Figure 8: Ablation study of MLP on CIFAR10/CIFAR100 (images are flattened into vectors). Default model: 10 layers, width 1000, batch size 256.

	BK	Non-DP	GhostClip	Opacus
Time complexity	$6B \sum_l T_{(l)} p_{(l)} d_{(l)} + \sum_l \left(\mathbb{I}\{2T_{(l)}^2 < p_{(l)} d_{(l)}\} \cdot 2B \sum_l T_{(l)}^2 (p_{(l)} + d_{(l)}) \right)$	$6B \sum_l T_{(l)} p_{(l)} d_{(l)}$	$10B \sum_l T_{(l)} p_{(l)} d_{(l)} + 2B \sum_l T_{(l)}^2 (p_{(l)} + d_{(l)})$	$8B \sum_l T_{(l)} p_{(l)} d_{(l)}$
RoBERTa-base	$15.3 * 10^{12}$	$13.1 * 10^{12} (0.86\times)$	$24.1 * 10^{12} (1.57\times)$	$17.5 * 10^{12} (1.14\times)$
RoBERTa-large	$52.3 * 10^{12}$	$46.5 * 10^{12} (0.89\times)$	$83.3 * 10^{12} (1.59\times)$	$62.0 * 10^{12} (1.18\times)$
ViT-base	$11.2 * 10^{12}$	$10.1 * 10^{12} (0.90\times)$	$18.0 * 10^{12} (1.60\times)$	$13.5 * 10^{12} (1.20\times)$
ViT-large	$38.8 * 10^{12}$	$35.8 * 10^{12} (0.92\times)$	$62.7 * 10^{12} (1.61\times)$	$47.7 * 10^{12} (1.23\times)$
BEiT-large	$29.1 * 10^{12}$	$26.9 * 10^{12} (0.92\times)$	$47.1 * 10^{12} (1.61\times)$	$35.8 * 10^{12} (1.23\times)$
Space complexity	$B \sum_l \min\{2T_{(l)}^2, p_{(l)} d_{(l)}\} + B \sum_l T_{(l)} (3d_{(l)} + p_{(l)})$	$\sum_l p_{(l)} d_{(l)} + B \sum_l T_{(l)} (3d_{(l)} + p_{(l)})$	$2B \sum_l T_{(l)}^2 + B \sum_l T_{(l)} (3d_{(l)} + p_{(l)})$	$B \sum_l p_{(l)} d_{(l)} + B \sum_l T_{(l)} (3d_{(l)} + p_{(l)})$
RoBERTa-base	$5.3 * 10^9$	$4.5 * 10^9 (0.84\times)$	$5.3 * 10^9 (1.00\times)$	$16.7 * 10^9 (3.17\times)$
RoBERTa-large	$13.3 * 10^9$	$11.8 * 10^9 (0.88\times)$	$13.3 * 10^9 (1.00\times)$	$46.9 * 10^9 (3.52\times)$
ViT-base	$3.3 * 10^9$	$3.0 * 10^9 (0.91\times)$	$3.3 * 10^9 (1.00\times)$	$11.5 * 10^9 (3.47\times)$
ViT-large	$8.5 * 10^9$	$8.1 * 10^9 (0.95\times)$	$8.5 * 10^9 (1.00\times)$	$38.1 * 10^9 (4.46\times)$
BEiT-large	$6.4 * 10^9$	$6.1 * 10^9 (0.95\times)$	$6.4 * 10^9 (1.00\times)$	$28.6 * 10^9 (4.46\times)$

Table 8: Time (upper half) and space (lower half) complexity of implementations ($B = 100$). For RoBERTa and GLUE datasets, $T = 256$; we use BK base (\equiv BK-MixOpt). For vision transformers and ImageNet, $T = 224 \times 224$; we use BK-MixOpt. We mark the ratio of complexity to BK in ().

Model	Algorithm	Maximum batch size	Time/Epoch	Maximum throughput	Speedup by BK
RoBERTa-large SST-2	BK (ours)	41	13:33	83	—
	Non-private	51	9:50	114	$0.73\times$
	GhostClip	48	17:34	64	$1.30\times$
	Opacus	16	22:30	50	$1.66\times$
RoBERTa-large QNLI	BK (ours)	41	20:14	86	—
	Non-private	51	15:33	112	$0.77\times$
	GhostClip	48	27:45	63	$1.37\times$
	Opacus	16	35:03	50	$1.73\times$
RoBERTa-large QQP	BK (ours)	41	70:04	87	—
	Non-private	51	53:42	113	$0.77\times$
	GhostClip	48	95:09	64	$1.36\times$
	Opacus	16	137:00	44	$1.96\times$
RoBERTa-large MNLI	BK (ours)	41	77:07	85	—
	Non-private	51	58:02	113	$0.75\times$
	GhostClip	48	103:30	63	$1.34\times$
	Opacus	16	134:30	49	$1.75\times$
GPT2	BK (ours)	149	2:22	296	—
	Non-private	157	1:47	393	$0.75\times$
	GhostClip	156	2:54	242	$1.22\times$
	Opacus	43	5:03	139	$2.13\times$
GPT2-medium	BK (ours)	69	5:25	129	—
	Non-private	70	4:05	172	$0.75\times$
	GhostClip	70	6:46	104	$1.24\times$
	Opacus	15	14:22	49	$2.63\times$
GPT2-large	BK (ours)	29	11:20	62	—
	Non-private	29	8:16	85	$0.73\times$
	GhostClip	29	13:56	50	$1.24\times$
	Opacus	5	44:05	16	$3.88\times$
BEiT-large	BK (ours)	96	6:35	127	—
	Non-private	98	4:55	169	$0.76\times$
	GhostClip	95	8:53	93	$1.33\times$
	Opacus	5	4:12:00	3	$38.3\times$

Table 9: Extension of Table 1. Note that CIFAR means both CIFAR10 and CIFAR100. Performance of GPT2 on E2E dataset (same setting as Li et al. (2021); Bu et al. (2022b)).

Model	Mixed ghost norm (MGN)	Per-sample grad instantiation		Ghost norm	
	$\sum_l \min\{2T_{(l)}^2, p_{(l)}d_{(l)}\}$	$(\sum_l p_{(l)}d_{(l)}; \# \text{ param})$	Saving by MGN	$(\sum_l 2T_{(l)}^2 = 2H_{\text{out}}^2 W_{\text{out}}^2)$	Saving by MGN
ResNet18	1.0M	11.5M	11.5×	399M	399×
ResNet34	2.3M	21.6M	9.4×	444M	194×
ResNet50	2.8M	22.7M	8.0×	528M	186×
ResNet101	6.8M	41.7M	6.2×	532M	79×
ResNet152	10.9	57.3M	5.3×	549M	51×
DenseNet121	4.1M	7.9M	1.9×	605M	147×
DenseNet161	9.0M	28.5M	3.2×	607M	67×
DenseNet201	7.0M	19.8M	2.8×	609M	87×
Wide ResNet50	5.6M	66.0M	11.7×	528M	93×
Wide ResNet101	9.6M	124.0M	13.0×	531M	56×
vit_tiny_patch16_224	3.3M	5.6M	1.7×	3.8M	1.1×
vit_small_patch16_224	3.8M	21.9M	5.8×	13.8M	1.0×
vit_base_patch16_224	3.8M	86.3M	22.7×	3.8M	1.0×
vit_large_patch16_224	7.5M	303.8M	40.4×	7.5M	1.0×
crossvit_tiny_240	4.0M	6.9M	1.7×	10.4M	2.6×
crossvit_small_240	5.9M	26.6M	4.5×	10.4M	1.8×
crossvit_base_240	8.7M	104.5M	12.1×	10.4M	1.2×
convnext_small	12.4M	50.1M	4.0×	214M	17×
convnext_base	14.3M	88.4M	6.2×	214M	15×
convnext_large	19.8M	197.5M	10.0×	214M	11×
deit_tiny_patch16_224	3.3M	5.6M	1.7×	3.8M	1.1×
deit_small_patch16_224	3.8M	21.9M	5.8×	3.8M	1.0×
deit_base_patch16_224	3.8M	86.3M	22.7×	3.8M	1.0×
beit_base_patch16_224	2.9M	86.3M	29.8×	2.9M	1.0×
beit_large_patch16_224	5.7M	303.8M	53.3×	5.7M	1.0×

Table 10: Space complexity of computing per-sample gradient norm, on ImageNet image (224×224). The saving by the mixed ghost norm, adopted in BK-MixGhostClip and BK-MixOpt, is substantial.

G Effect of hybridization: layerwise space complexity

We demonstrate the effect of hybridization (i.e. mixed ghost norm Bu et al. (2022a)) on the computation of per-sample gradient norm. We consider the moderate feature dimension and the high feature dimension, respectively. We conclude that ghost norm trick (adopted in GhostClip and BK) is favored closer to the input layer, whereas the per-sample gradient instantiation (adopted in Opacus and FastGradClip) is favored closer to the output layer.

G.1 Effect by model achitecture ($T = 224 \times 224$)

Generally speaking, CNN can benefit from hybridization, but vision transformers may not (unless the feature dimension is high, see next section for BEiT).

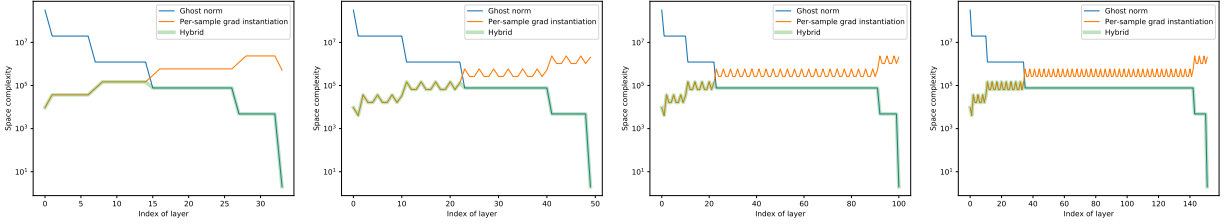


Figure 9: Layerwise space complexity of computing the per-sample gradient norm. Left to right: ResNet 34/50/101/152.

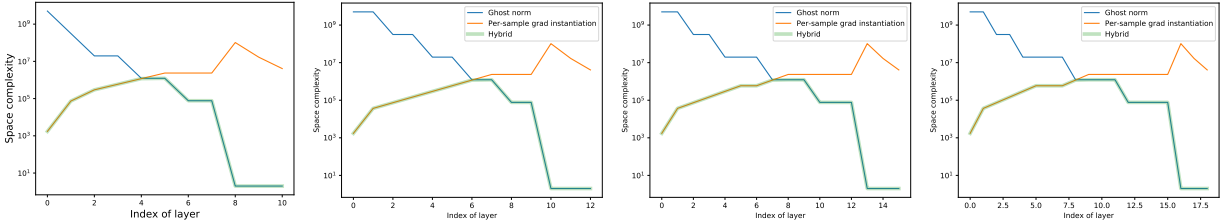


Figure 10: Layerwise space complexity of computing the per-sample gradient norm. Left to right: VGG 11/13/16/19.

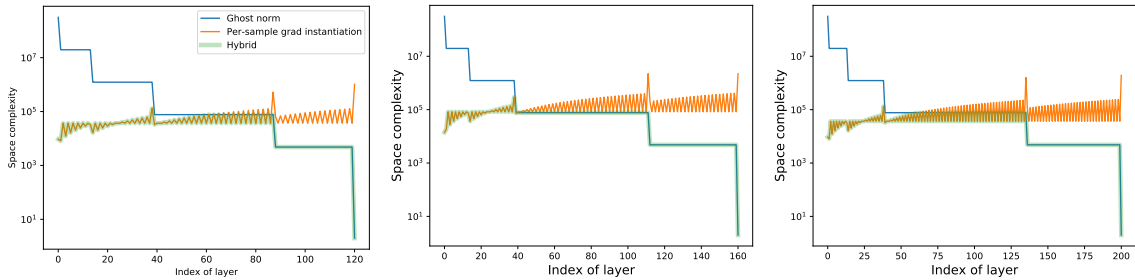


Figure 11: Layerwise space complexity of computing the per-sample gradient norm. Left to right: DenseNet 121/161/201.

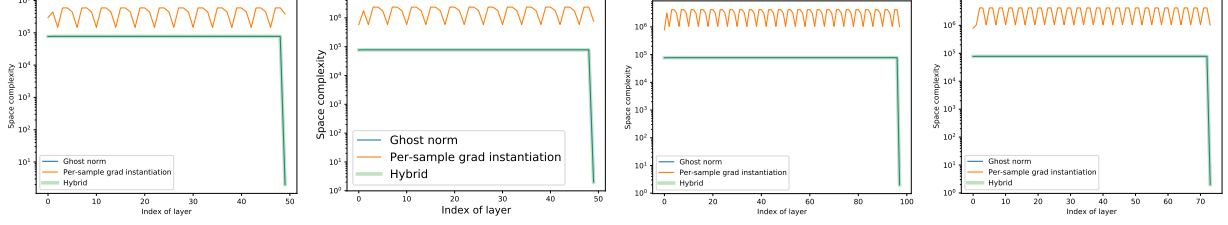


Figure 12: Layerwise space complexity of computing the per-sample gradient norm. Left to right: ViT small/base/large, and BEiT-large.

G.2 Effect by feature dimension ($T = 32^2/224^2/512^2$)

Generally speaking, higher feature dimension requires a deeper threshold, after which the per-sample gradient instantiation is not preferred. That is, high dimensional data does not prefer ghost norm. This pattern even holds for vision transformers, on which MixGhostClip/BK-MixGhostClip is equivalent to GhostClip/BK for low feature dimension.

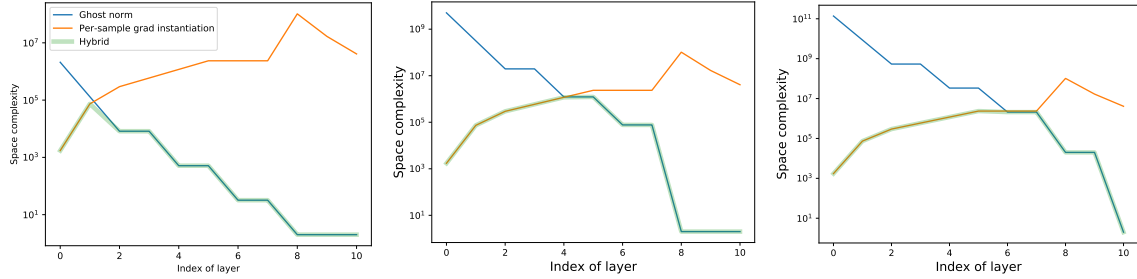


Figure 13: Layerwise space complexity of computing the per-sample gradient norm in VGG11.

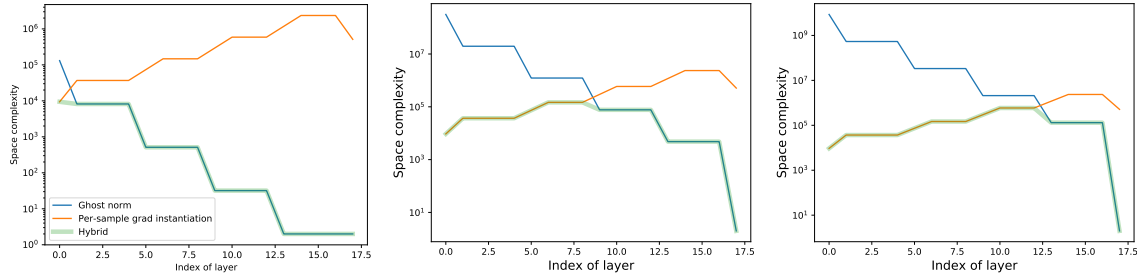


Figure 14: Layerwise space complexity of computing the per-sample gradient norm in ResNet18.

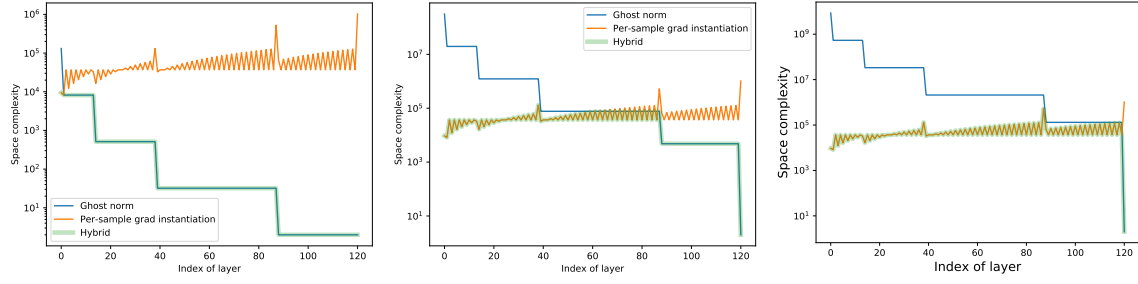


Figure 15: Layerwise space complexity of computing the per-sample gradient norm in DenseNet121.

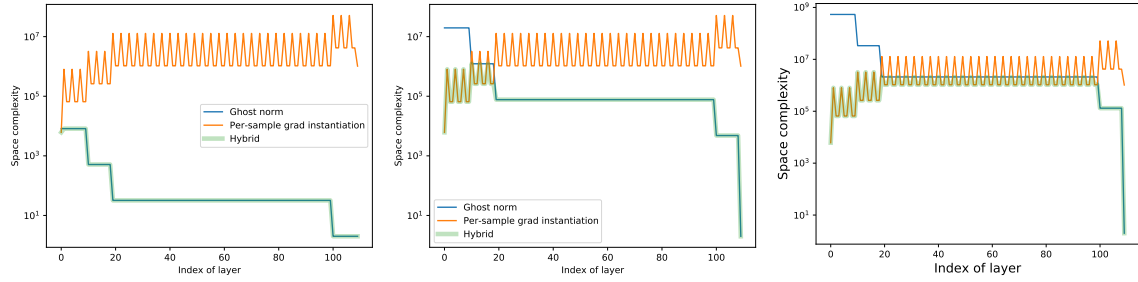


Figure 16: Layerwise space complexity of computing the per-sample gradient norm in ConvNeXT.

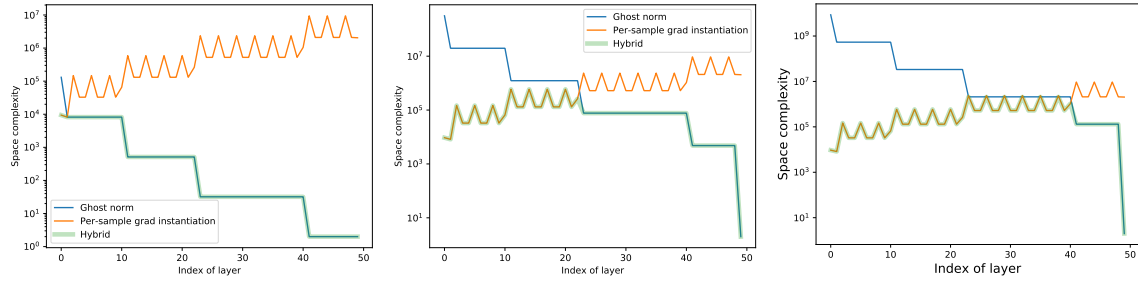


Figure 17: Layerwise space complexity of computing the per-sample gradient norm in Wide ResNet50.

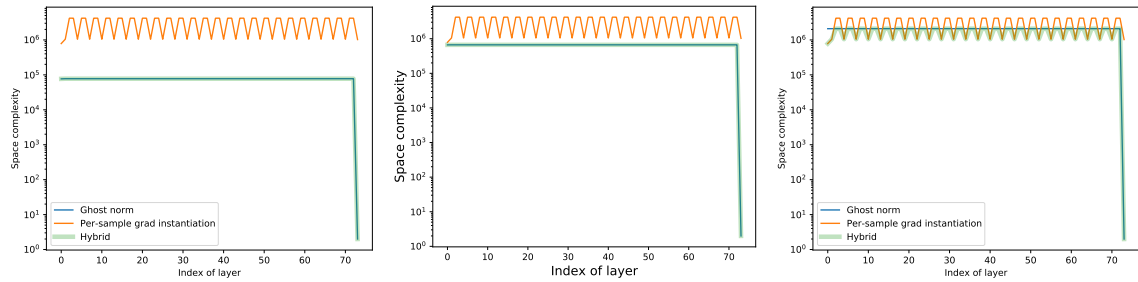


Figure 18: Layerwise space complexity of computing the per-sample gradient norm in BEiT-large.